AD_____

Award Number: W81XWH-10-1-0773

TITLE: Mechanical Loading for Peripheral Nerve Stabilization and Regeneration

PRINCIPAL INVESTIGATOR: Sameer B. Shah, Ph.D.

CONTRACTING ORGANIZATION: University of California, San Diego
La Jolla, CA 92093-0934

REPORT DATE: April 2013

TYPE OF REPORT: Final Report

PREPARED FOR: U.S. Army Medical Research and Materiel Command
Fort Detrick, Maryland 21702-5012

REPORT DOCUMENTATION PAGE

Form Approved
OMB No. 0704-0188

1. REPORT DATE	2. REPORT TYPE	3. DATES COVERED
April 2013	FInal	15 September 2010–14 March 2013

4. TITLE AND SUBTITLE
Mechanical Loading for Peripheral Nerve Stabilization and Regeneration

5a. CONTRACT NUMBER

5b. GRANT NUMBER
W81XWH-10-1-0773

5c. PROGRAM ELEMENT NUMBER

6. AUTHOR(S)
Sameer B. Shah, Ph.D. (PI)
Ting-Hsien Chuang, Ph.D. (Postdoc)
Robin Wilson (Student Research Scientist)

5d. PROJECT NUMBER

5e. TASK NUMBER

5f. WORK UNIT NUMBER

7. PERFORMING ORGANIZATION NAME(S) AND ADDRESS(ES)
University of California, San Diego
9500 Gilman Drive, MC 0934
La Jolla, CA 92093-0934

8. PERFORMING ORGANIZATION REPORT NUMBER

9. SPONSORING / MONITORING AGENCY NAME(S) AND ADDRESS(ES)
U.S. Army Medical Research and Materiel Command
Fort Detrick, Maryland 21702-5012

10. SPONSOR/MONITOR'S ACRONYM(S)

11. SPONSOR/MONITOR'S REPORT NUMBER(S)

12. DISTRIBUTION / AVAILABILITY STATEMENT
Approved for Public Release; Distribution Unlimited

13. SUPPLEMENTARY NOTES

14. ABSTRACT
Peripheral nerve damage is one consequence of injury to the extremities of soldiers by improvised explosive devices (IEDs). The degree of functional recovery from peripheral nerve damage is often poor, particularly for severed nerves. The result can be impaired motor function, sensory loss, and chronic pain with inappropriate autonomic responses. Consequently, strategies for enhancing nervous function are of high military relevance. Towards the development of more effective nerve regeneration strategies, this proposal addresses the hypothesis that moderate tensile loading (stretch) of peripheral nerves can stabilize nerve degradation and also promote accelerated regeneration. Our project aims are to 1) To examine the impact of low levels of tensile loading on the Wallerian degeneration of proximal and distal stumps of severed peripheral nerves and 2) To examine the impact of moderate levels of tensile loading on promoting the outgrowth and functional connectivity of severed peripheral nerves. To meet these aims, in the final project period, based on results from initial in vivo implantations, we completed characterization of proximal and distal nerve stumps following 3-6 weeks of device implantation. No adverse effects were observed following 20% initial deformation, suggesting that, at minimum, tension provides a head start for nerve regeneration. Long-term survival surgeries will be required to formally test whether functional recovery is accelerated.

15. SUBJECT TERMS
Peripheral nerve, nerve regeneration, biomedical device, biomechanics, rat nerve injury

16. SECURITY CLASSIFICATION OF:			17. LIMITATION OF ABSTRACT	18. NUMBER OF PAGES	19a. NAME OF RESPONSIBLE PERSON
a. REPORT	b. ABSTRACT	c. THIS PAGE			USAMRMC
U	U	U	UU		19b. TELEPHONE NUMBER *(include area code)*

Table of Contents

INTRODUCTION

Peripheral nerve damage is one consequence of injury to the extremities of soldiers by improvised explosive devices (IEDs) [1, 2]. The degree of functional recovery from peripheral nerve damage is often poor, particularly for severed nerves. The result can be impaired motor function, sensory loss, and chronic pain with inappropriate autonomic responses. Consequently, strategies for enhancing nervous function are of high military relevance. A variety of chemical guidance cues and synthetic scaffolds have been incorporated into strategies for neuronal regeneration and outgrowth, but have not yet yielded adequate growth rates or been limited by insufficient source tissue[3]. The mechanical environment of a neuron is a key determinant of its growth and function [4-9]. This aspect of neuronal outgrowth has been underutilized in nerve regeneration strategies.

Towards the development of more effective nerve regeneration strategies, this proposal addresses the hypothesis that moderate tensile loading of peripheral nerves can stabilize nerve degradation and also promote accelerated regeneration. This hypothesis is motivated by observations that nerves are under tension physiologically, indicated by elastic recoil following transection, and also by observations that moderate levels of tensile loading can accelerate neuronal growth, both in vitro and in vivo [4-9]. Our project aims are to *1) To examine the impact of low levels of tensile loading on the Wallerian degeneration of proximal and distal stumps of severed peripheral nerves and 2) To examine the impact of moderate levels of tensile loading on promoting the outgrowth and functional connectivity of severed peripheral nerves.*

In our final project period, we implanted two different biomedical devices, one a fixed length and one extensible into a rat sciatic nerve defect. We describe in the body of this report our characterization of the in vivo response.

BODY

Completed milestones and specific outcomes/comparisons for each milestone based on the original statement of work are summarized below. We have also included the remaining milestones as originally listed, as well as unanticipated results, which were detailed in previous annual reports and are now expanded upon in the final report. It should be noted that funding was spent out shortly after the previous annual report. A no cost extension (NCE) was granted to extend 18 months of funding to 30 months of funding; however, funds were in reality depleted in 25 months. Results reflect progress both during period with funding and subsequent progress during an unfunded period, but nevertheless relevant to the scope of the grant.

Detailed results from our design, fabrication and implantation of our devices are below the completed milestones. Figure 1 reflects images associated with unanticipated deviations, Figures 2-8 are also summarized in the appended reprint of our accepted publication. Figures 9-10 reflect initial characterization of new datasets that are being prepared for submission.

Completed milestones per statement of work (SOW) revised following transfer from Maryland to UCSD (same as original, with modifications for UCSD IACUC approval and ACURO animal protocol approval)

Milestones and deliverables for Animal protocols:

0.1. Approval of animal protocol by UCSD IACUC (APPROVED – UCSD IACUC PROTOCOL S11274).

0.2. Approval of animal protocol by ACURO (APPROVED)

Milestones and deliverables for Aim 1 (fixed nerve length):

1.1. Successful fabrication and in situ testing of nerve stabilizing device.
   a. Fabrication of collagen matrix guidance channel
   b. Fabrication of poly methyl methacrylate (PMMA) fixator
   c. Assembly of device within nerve gap created in rat cadaver, including coupling of guidance channel to nerve stumps with spiral cuff

1.2. Successful in vivo implantation of nerve stabilizing device for short durations (48 hours).
   a. Implantation of device into anesthetized animal
   b. Removal of device and tissue harvest at 48 hour time point
   c. Freezing and sectioning of tissue for analysis in Milestone 1.4

1.3. Successful in vivo implantation of nerve stabilizing device for longer durations (1-6 weeks).
   a. Implantation of device into anesthetized animal
   b. Removal of device and tissue harvest at 1, 3, and 6 week time points
   c. Freezing and sectioning of tissue for analysis in Milestone 1.4

1.4. Comparison of nerve outgrowth, cytoskeletal stability, organelle accumulation, and myelination between 10 mm (no device), 10 mm (device) at 1 and 3 week time points.

Milestones and deliverables for Aim 2:

2.1. Successful fabrication and in situ testing of nerve lengthening devices with both actuation mechanisms.
   a. Fabrication of collagen matrix guidance channel (same as for Aim 1)
   b. Fabrication of PMMA fixators, including actuation assemblies
   c. Assembly of device within nerve gap created in rat cadaver
   d. Successful application of nerve stretch with at least one of the actuation devices in a rat cadaver

2.2. Successful in vivo implantation of nerve lengthening device for longer durations (1-6 weeks)
   a. Implantation of devices into anesthetized animals
   b. Removal of device and tissue harvest at 1 week time points
   c. Freezing and sectioning of tissue for analysis in Milestone 2.3

Remaining milestones per original SOW – see pitfalls and deviations from original strategy.

Remaining milestones and deliverables for Aim 1 (fixed nerve length):

1.4. Comparison of nerve outgrowth, cytoskeletal stability, organelle accumulation, and myelination between 10 mm (no device), 10 mm (device), and 15 mm (device) groups at all four time points. The following measurements will be compared using a 2-way analysis of variance (ANOVA), considering gap length vs. time.
   a. Comparison of nerve outgrowth across groups: distance of farthest neuron terminal beyond original stump ending or, if applicable, distance over which degeneration has occurred.
   b. Comparison of cytoskeletal stability: proportion of axonal length containing properly aligned neurofilament, tubulin, or actin staining. Alternately, the density of cytoskeleton-containing spheroids (indicating instability) along the nerve.
   c. Comparison of organelle accumulation: density of mitochondrial or Calcitonin gene related peptide (CGRP) staining in stump ending.
   d. Comparison of myelination: nerve fiber diameter and myelin diameter. Position along nerve length may be a covariate (analysis of covariance (ANCOVA)).

Remaining milestones and deliverables for Aim 2 (actuation devices):

2.2. Successful in vivo implantation of nerve lengthening device for longer durations (1-6 weeks)
   d. Removal of device and tissue harvest at 3, and 6 week time points
   e. Freezing and sectioning of tissue for analysis in Milestone 2.4

2.3 Statistical comparison of nerve outgrowth, cytoskeletal stability, organelle accumulation, myelination, and toe spreading (function) between 10 mm (no device), 10 mm (device), and 15 mm (device) groups for both actuation mechanisms at all three time points.

Pitfalls and deviations from original strategy

(Entire project period)

Period 1: We have made two minor deviations in the design of the fixator device, both regarding material choice. Instead of PMMA, the backbone and telescoping mechanisms of the devices have been fabricated out of stainless steel, which is also United States Food and Drug Administration (FDA) approved for implantation. The advantages of this material are the ready availability of prefabricated stainless steel rods and tubes of narrow diameter. In addition, due to the unpredictability of collagen expansion following hydration, we have fabricated tissue engineered guidance channels from poly(lactic-co-glycolic acid) (PLGA), which is also an FDA-approved biocompatible scaffold used previously in a nerve regeneration model [10, 11].

Period 2:

The PI has relocated his laboratory to UCSD, within the department of Orthopaedic Surgery. Collaborations with relevant investigators at the University of Maryland and at the FDA remain intact, and the key postdoc working on the project, Dr. Ting-Hsien Chuang, also moved to UCSD. As a result of this change of institution, animal studies were placed on hold until the approval of the animal protocol at UCSD (and subsequent approval by ACURO). A no-cost extension was requested and granted through April 2013.

Observations from the large number in vivo implantations since the initial project period were quite informative. Feasibility was demonstrated for long-term implantations for both static and dynamics devices. Not surprisingly for a novel technology, though, several minor design changes were required to improve the performance of the device.

First, devices translated more than expected, despite the tight constraints of the nerve bed. This resulted in an inability to ascertain the exact distribution of strain in the proximal and distal stump. Consequently, simple anchors (1 mm in length) into the underlying muscle were fabricated out of stainless steel. These successfully tethered the device to the muscle bed, prevented translation, and confirmed the accurate application of desired stain onto the nerve stumps.

Second, a simple non-ratchet lengthening device was tested, and a ratchet-based lengthening device was designed. After in situ testing, it was apparent that we could achieve the benefits of both devices by simply extending the guidewire housing slightly extracorporeally, to provide a fixed frame of reference against which the guidewire may be actuated. The simpler device is adequate to test our hypotheses, and a request will be made to modify the SOW accordingly .

Modified devices are being used across all implantation groups, and do not appear to require an SOW modification, given the current language of the SOW.

Third, 15mm gaps have been determined to be unfeasible for device implantation within the rat. This length was chosen based on literature reports of passive nerve scaffolds being implanted in such gaps, but in the typical large adult rat, including those >400g, this length requires either the severing of individual distal branches of the sciatic nerve or more invasive dissection further proximally. In either case, sufficient nerve does not exist for cuff deployment and proper device orientation. Therefore, comparison of nerve outgrowth, was made between 10 mm (no device), 10 mm (device, 10% strain; physiological), and 10 mm (device, 20% strain; superphysiological) groups at all four time points.

Periods 2-3:
Fourth, the biggest unanticipated hurdle was the surprisingly high rate of autotagy (self-mutilation) among injured rats at time points >2 weeks. We did not observe this problem at earlier time points, for unknown reasons. However, up to 40% of animals demonstrated some form of toe or hindlimb chewing, rendering these animals un-analyzable. While this outcome is not unheard of for nerve (or spinal cord) injury, it was nonetheless unanticipated given the large number of short-time point surgeries completed. Consultation with the veterinary staff and a deeper examination of autotagy literature led to our recent modification of pre-op and post-op dosages for buprenorphine and metacam, extending the latter to the experimental endpoint rather than cutting it off at 1.5 weeks, as originally recommended by the veterinary staff. This phenomenon is often equated to a phantom limb phenomenon in humans; therefore, it may not be a response to pain, in animals. Therefore, in addition, bitter apple delivered within a New Skin liquid bandage will also be applied topically, as a deterrent. This constituted a minor amendment within our IACUC, and a similar request will be made to ACURO. The downside of the observed autotagy was the inability to use many of these animals for analysis; these experiments are being repeated under new dosing guidelines.

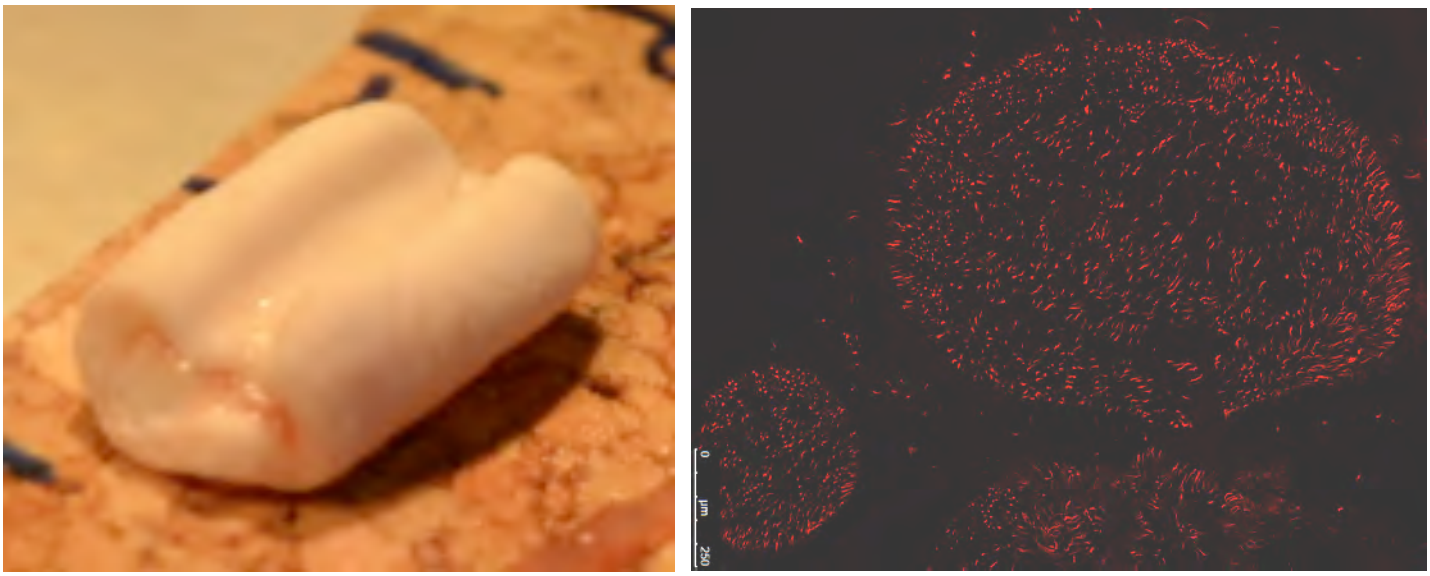

Figure 1. (Left) Collapsed PLGA scaffold after 6 weeks blocked outgrowth of most nerves. (Right) However SMI-31 staining of Phospho-neurofilaments (axons) in the distal stump indicated that regeneration did occur across the few scaffolds that did stay intact.

Fifth, over longer implantation periods (3-6 weeks), PLGA scaffolds collapsed (Fig. 1A). Though qualitative growth was

observed across the nerve gap within 6 weeks for all three static groups (Fig. 1B), quantitative assessment of regrwoth rates were not suitable for statistical comparison, and we were unable to quantify organelle accumulation, cytoskeletal stability, or myelination. This being said, the fact that none of these phenomea seemed to be affected at 3 weeks suggests that it is unlikely that they would have occurred at 6 weeks. Similarly, we were also unable to assess motor functional recovery (i.e., toe spreading) due to tube collapse prior to 6 weeks. To address these issues, a non-tubular scaffold, such as decellularized nerve grafts, will be proposed for subsequent work. Nevertheless, we are cautiously optimistic that (i) there were no adverse consequences of lengthening; and (ii) there were no feasibility barriers (other than autotagy and PLGA scaffold collapse) to implementation of this strategy in future work. We will publish results from the 3-week time point, and work to secure funding for long-term survival studies.

Detailed results.

Device fabrication

The device is composed of three major components: self-sizing silicone spiral nerve cuffs, poly(lactic co-glycolic) acid (PLGA) nerve guidance channels (NGCs), and a mechanical backbone to which the cuffs and nerve guidance channels are attached (Fig. 2).

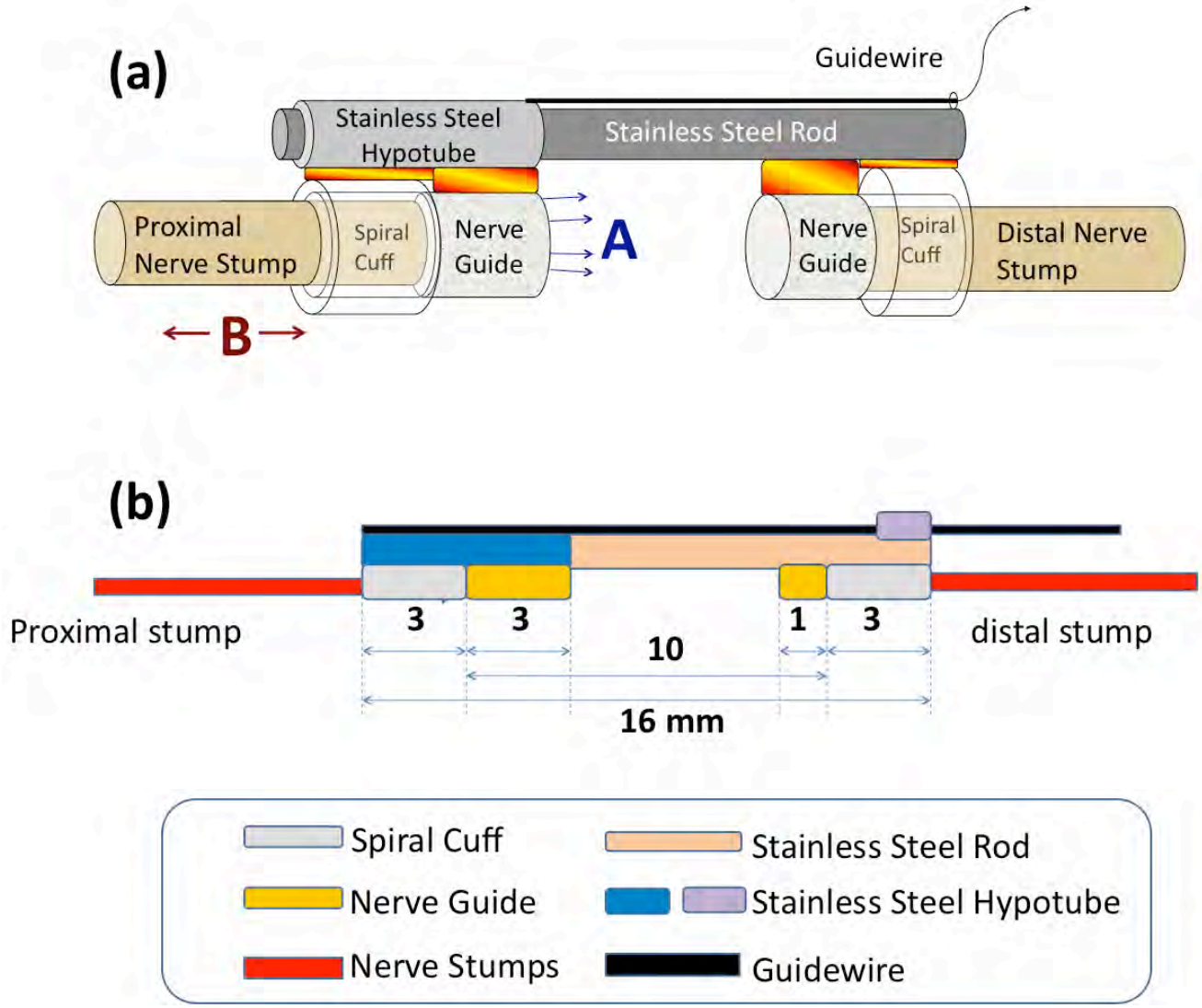

Figure 2. The nerve stretching device is composed of spiral nerve cuffs, PLGA nerve guidance channel and stainless steel backbone (a) Two regions of regeneration, A: Enhanced axonal outgrowth into a tissue engineered nerve guide/scaffold; B: Lengthening of intact regions of nerve stumps – cf. limb lengthening. (b) Dimension of the device

Spiral nerve cuffs

The fabrication of spiral nerve cuffs is shown in Fig 3a; two silicone sheets, one stretched to a specific strain, were glued together and clamped between two metal slabs. After curing, the compound sheet curled into spiral shape (Fig. 3b). In addition, the microgroove pattern was successfully transferred to the compound silicone sheet (Fig. 3c). The curled sheet was cut into small segments of 3 mm to serve as nerve cuffs. Measurements of the inner diameter of the spiral nerve cuffs showed a decreasing trend of inner diameter with increasing percent strain in the silicone sheet. In the test of efficacy of nerve gripping, cuffs of 70% and 100% pre-loaded strain (average inner diameter of 1.35mm and 0.85mm, respectively) successfully held the nerve without slippage, though self-sizing was more reliable in the 100% strain cuff. The inner surface of spiral nerve cuff was in close contact with the nerve stump but caused minimal nerve compression, based on observation at high magnification through a dissecting microscope. The 100% strain cuff was used in the following studies based on its reliable self-sizing to the nerve.

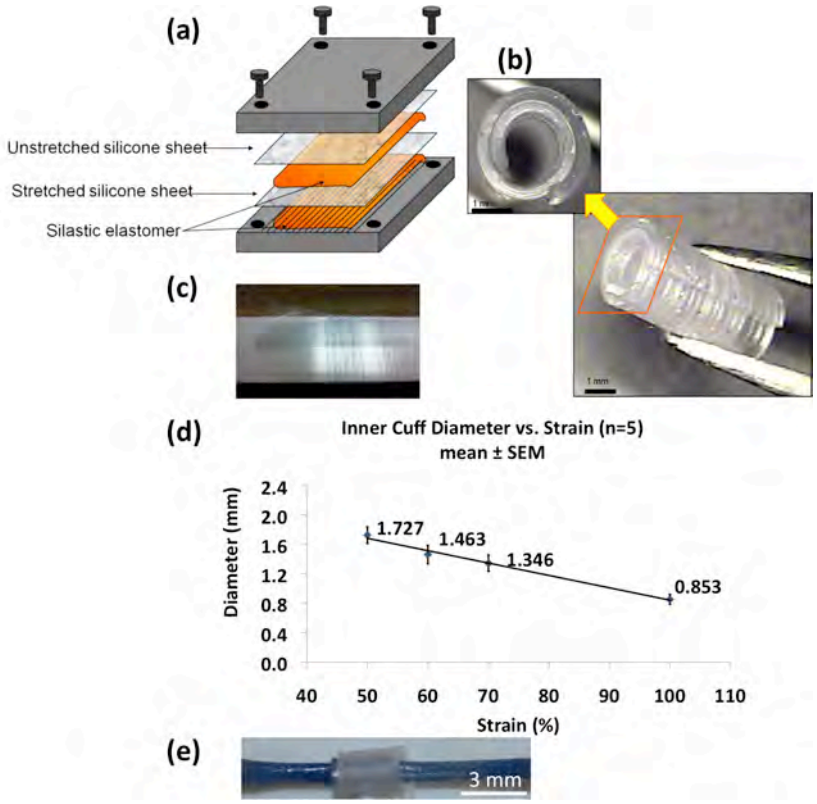

Figure 3. Fabrication and characterization of spiral nerve cuff (a) two layers of silicone sheets (with one being stretched) are glued together; (c) the microgroove pattern on the slab is transferred to the cuff; (b)the resultant curled nerve cuff after curing; (d) Inner diameter decreases with increasing % strain of pre-stretched silicone sheet; (e) sample ex vivo testing of trypan blue-labeled nerve in cuff revealed no appreciable compression or tethering.

PLGA nerve guidance channel

Due to phase separation, white solid state PLGA precipitated gradually onto the water-eluding alginate hydrogel. After retrieval of the alginate rod, a hollow PLGA tube was produced (Fig. 4a). The PLGA tube was then cut into small segments to serve as NGCs (Fig. 4b). As expected based on previous studies, cross-sectional scanning electron microcopy (SEM) images showed that the PLGA tubes had a porous structure (Fig. 4c). (42)

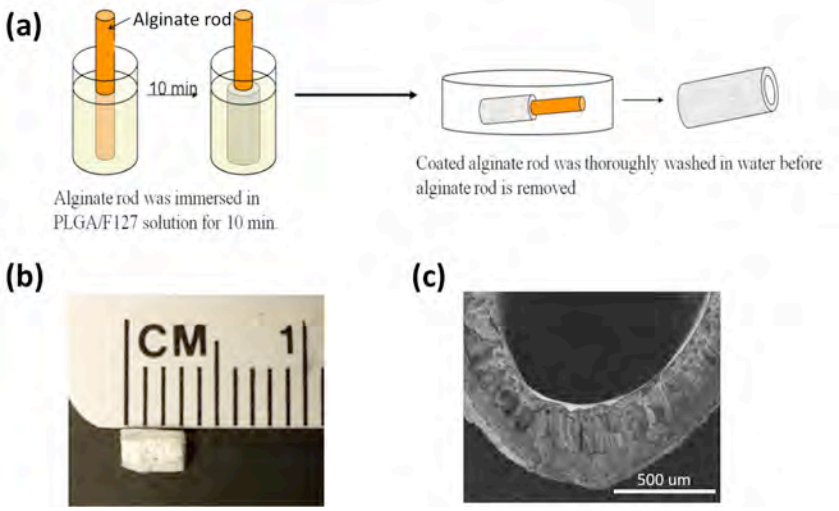

Figure 4. Fabrication of PLGA nerve guidance channel (a) Alginate rod was immersed in PLGA/Pluronic F127 solution for 10 min. Tubular PLGA layer is formed due to phase separation when water diffuses out the alginate rod; coated alginate rod was thoroughly washed in water before alginate rod is removed (b) PLGA tube is cut into short segments to serve as nerve guidance channel (c) Cross section SEM of PLGA tube.

PLGA cytotoxicity

For the test on extracts cytotoxicity method, SH-SY5Y cell fed with medium pre-incubated with PLGA showed similar morphology (Fig. 5a) to that of control (Fig. 5b). Live/Dead® cell viability assay also showed that only very few dead cells were present (Fig. 5c; Fig. 5d as control). From both results, no signs of cytotoxicity were observed. For cell proliferation on PLGA, the experimental group displayed no significant difference compared to the control group (Fig. 5e). For direct observation of morphology of cell grown on PLGA, wheat germ agglutinin (WGA) staining was performed. From the fluorescent microscopy images, we observed SH-SY5Y cells spread and extended outward. In light of neuronal preferences for a protein-coated substrate, we also seeded cells on PLGA coated with laminin. Neurites appeared more robust and cells appeared more dense on laminin-coated PLGA (Fig. 5f). Thus, overall, PLGA induced no significant effects on viability or morphology.

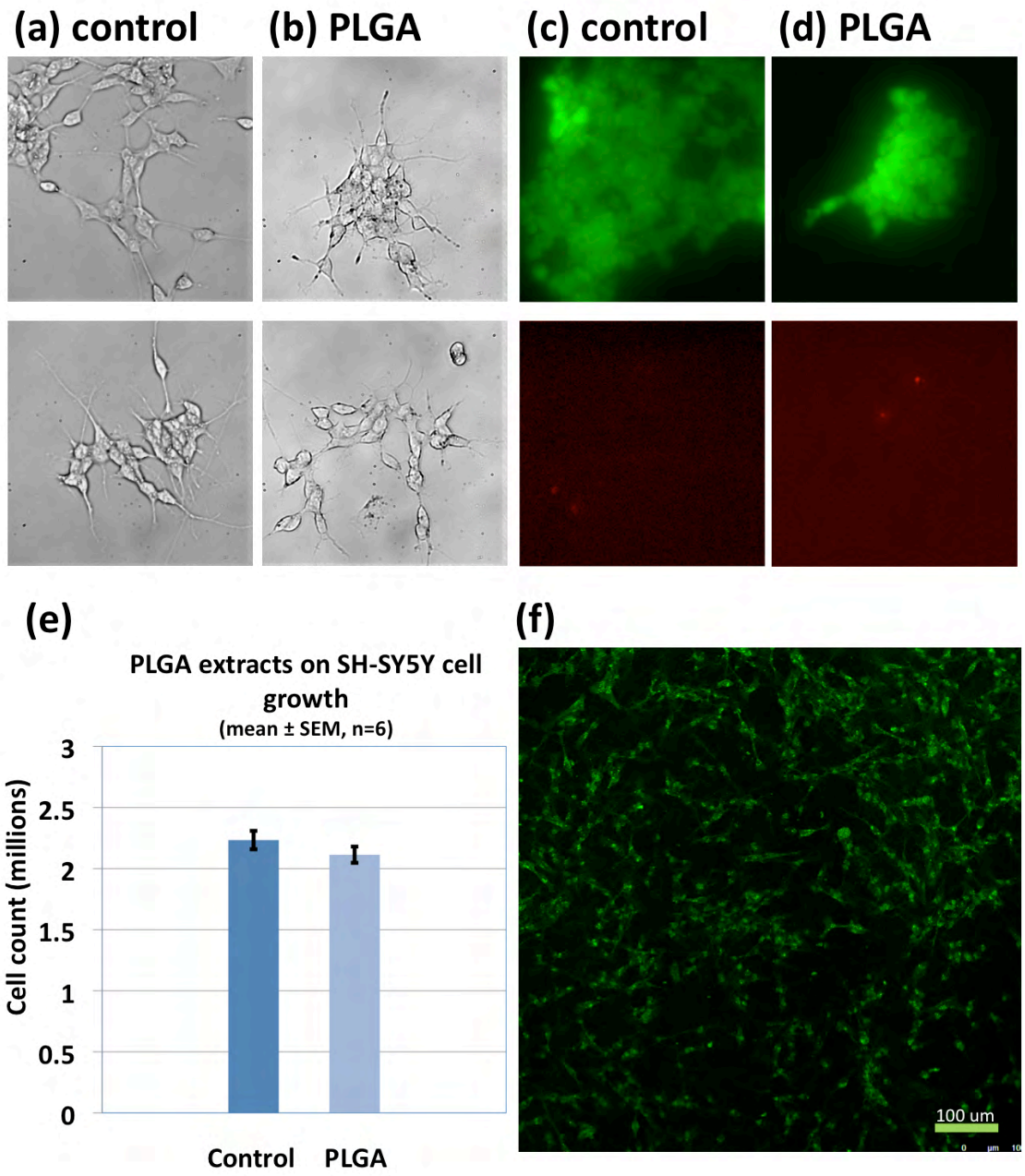

Figure 5. PLGA cytotoxicity. (a-d) Cells were fed with PLGA-incubated culture medium to test whether leachable substances from a PLGA scaffold would have cytotoxic effects on the cells. (a),(b) No signs of PLGA cytotoxicity was observed in terms of cell morphology; (c),(d) Live/Dead® cell viability assay indicated very few dead cells; (e) No statistical difference was found between control and PLGA group, p=0.05. (f) Visualization of morphology of cells grown on laminin-coated PLGA by fluorescent wheat germ agglutinin staining of cell membranes. SH-SY5Y cells attached, spread and proliferated on laminin-coated PLGA.

In situ implantation

The assembled device is shown *ex vivo* in Fig. 6a (before stretching nerve) and Fig. 6b (after stretching nerve). Deployment of the device was first performed in a rat cadaver. The device was implanted appositional to the transected nerve with the nerve stumps wrapped into the spiral cuffs (Fig. 6c). By pulling the guidewire attached to the hypotube sliding over the rod, the nerve stump of proximal end was successfully stretched and placed under tension (Fig. 6d). Following positioning, to prevent translation, the device was fixed to the underlying muscle with medical grade super glue or stainless steel anchors.

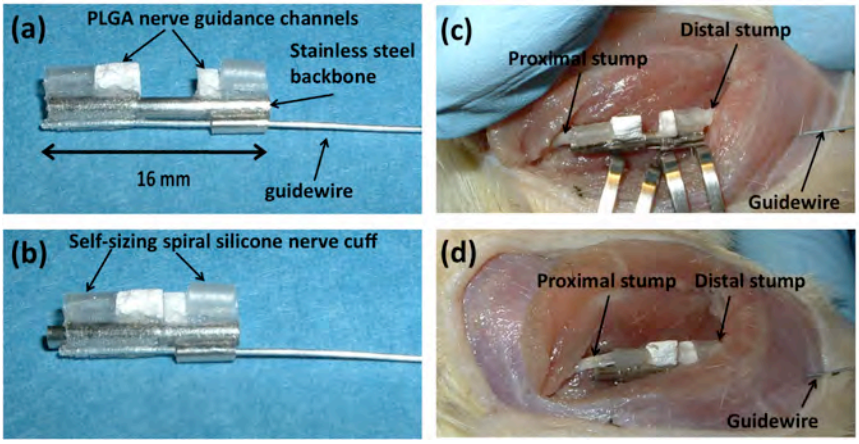

Figure 6. Demonstration of slip-free nerve deformation ex vivo. (a-b) device fully extended and maximally actuated, ex vivo. (c-d) fully extended device and actuated device in a rat sciatic nerve defect. Note that implanted device can stretch the nerve stumps 6mm without slippage.

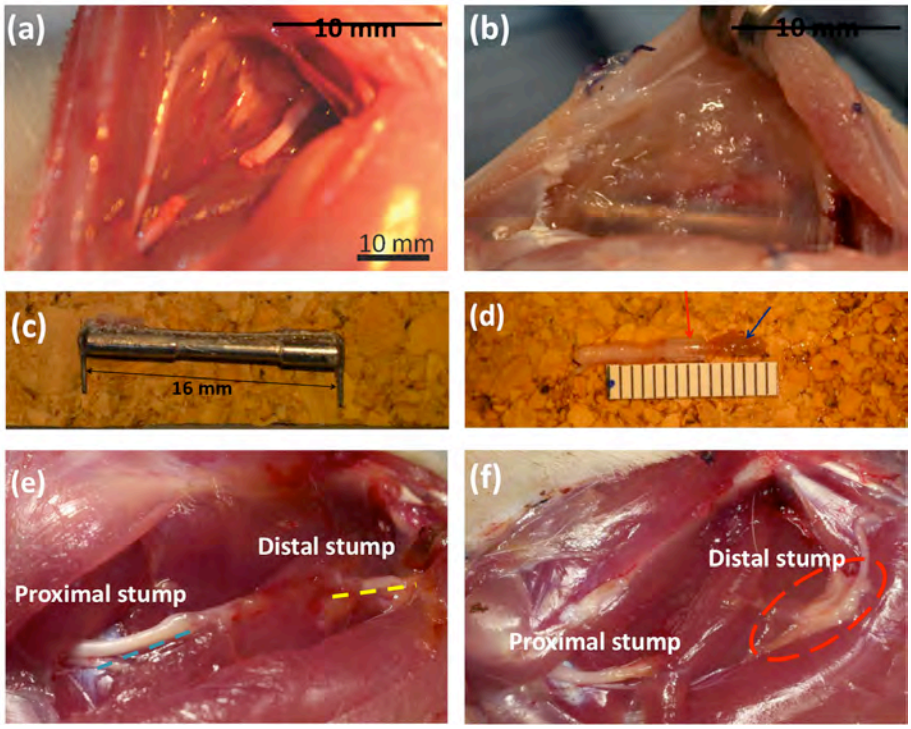

Figure 7. Response to 2-week implantation of device (a) A nerve gap was created by removal of 10 mm segment from the rat sciatic nerve. (b) Following two weeks of implantation, minor fibrosis was observed at the implantation site. (c) The stainless steel backbone was extracted cleanly at two weeks. (d) The proximal stump was still securely held by the nerve cuff (red arrow), and the regenerating tip extended beyond the cuff ~6mm (blue arrow). (e-f) In the absence of device implantation the two stumps remained disconnected and misaligned. A bulge was observed at the proximal stump and the degenerating distal stump appeared fused with surrounding fatty/connective tissue.

In vivo implantation

We then tested whether the device enabled nerve regeneration. The device was successfully deployed across a sciatic nerve defect (Fig. 7a) in anesthetized rats (n=5), demonstrating feasibility and repeatability of device implantation *in vivo*. In all animals, the animal tolerated the device for up to two weeks without obvious signs of infection. Slight fibrosis was observed (Fig 7b), but the device backbone was excised cleanly (Fig 7c), and both nerve stumps remained within the confinement of the cuffs without slippage. Within two weeks, the proximal stump extended 6 mm beyond the cuff (into the scaffold; Fig 7d). These results contrasted sharply with the response in non-device controls (n=3), which revealed a variable regenerative response, including misalignment, a bulging proximal stump, and considerable fatty infiltration and fibrosis distally (two examples in Fig 7e-f). Immunohistological assessment confirmed successful outgrowth of neurons

into the guidance channel as well as neuronal maturity, based on positive staining of phosphorylated neurofilaments (SMI-31 antibody) and aligned Schwann cells (S100 antibody) (Fig 8a-d). Such alignment and staining was similar to that in contralateral controls (Fig 8e-g). Consistent with this alignment of cytoskeletal proteins and myelinating cells, cytoskeletal, somewhat surprisingly, there was no evidence of organelle accumulation, including mitochondria, at the distal stump in any of the three treatment groups within the two-week period. This disproved our original hypothesis that an absence of tension resulted in abnormal organelle accumulation, a bulging distal stump, and cytoskeletal disarray. On the other hand, tension did not appear to create any damage either, confirming the nerve's ability to tolerate and adapt to moderate loads.

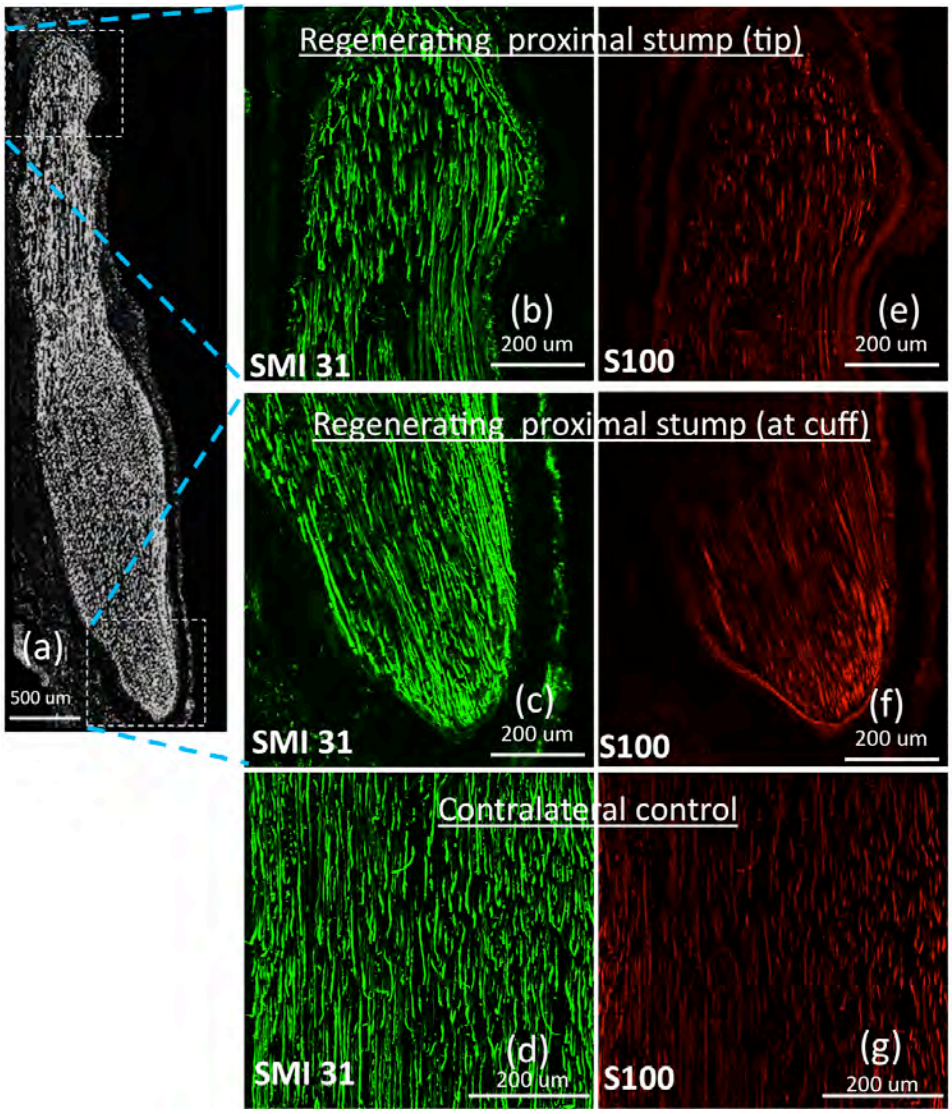

Figure 8. Evidence of regenerative neural outgrowth (a) the regenerating nerve extended ~6mm beyond the cuff, and was stained with anti-SMI-31 (a, b, c) and anti-S100 (e, f) antibodies, which labeled phosphorylated neurofilaments and Schwann cells, respectively. (d, g) The contralateral sciatic nerve was stained with the same two markers and served as a control.

Progress until this point is included in the attached journal publication. Progress below this point reflects preliminary analysis of collected data that will be included in a subsequent manuscript.

3 week survival surgery

We built upon our demonstration of successful nerve regeneration under tension with two additional studies. First, we compared the short-term morphological response of nerves to device-imposed tension. Using our device, nerves were fixed at initial strains of 0%, 10%, and 20% for 3 weeks (n = 4 per group). As expected, intra-epineurial (i.e., cumulative fascicular) area and axonal caliber within the proximal stump decreased with increasing strain (Figure 9), indicating that the nerve was indeed under tension for 3 weeks. Compellingly, the number and density of axons in the proximal stump was significantly greater in the 10% and 20% strain groups compared to nerves under no tension. That such a difference was detected in such a small sample size speaks to the magnitude of the effect. We will continue to probe influences of tension on both proximal and distal stumps with additional metrics. However, even by the most conservative interpretation, nerves strained by 20% have a ~4mm "head start" on regeneration compared to the tension-free group, with no apparent negative effects. In the second preliminary study, we successfully imposed a 10% strain (relative to initial length, ~1mm) every 2 days for 1 week after device implantation across a 10mm gap. At the end of one week, proximal and distal stumps abutted, confirming the feasibility of continuous nerve extension *in vivo* within a short window. No neuroma was visible. However, as 3 weeks is too early a time point to expect functional recovery, long term experiments must be performed to determine whether regenerating axons pass across to the distal stump, and whether muscle function is restored.

Even within 3 weeks, structural changes in the distal stump were apparent, and distinguished this region from the intact proximal stump. As expected, basal lamina within endoneurial tubes compacted (Figure 9D vs. C). Within time frames of less than 45 days, this compacted structure facilitates neural guidance. However, structural integrity of the extracellular matrix appears to progressively decay, both within the epineurium as well as within fascicular compartments (Figure 10C-D vs. Figure 10A-B). Gomorri trichrome labeling indicates some infiltration of connective tissue into fascicular compartments, as indicated by colorimetric thresholding of the Aniline blue connective tissue label (Figure 10D-E). These results are suggestive, but will be carefully quantified at each time point. However, such results do suggest that a more distal reconnectivity can only help the regenerative process, as distal integrity, necessary for pathfinding, is clearly compromised as early as three weeks.

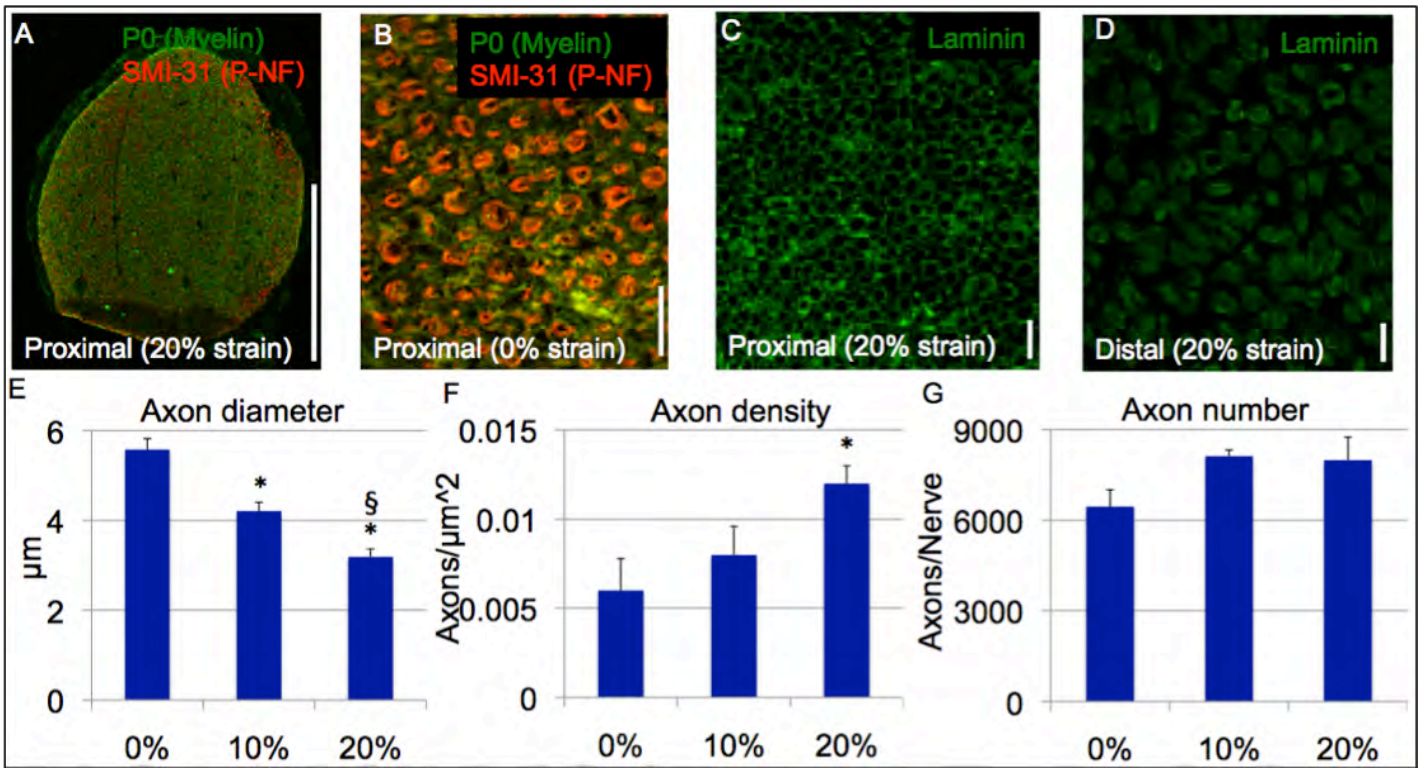

Figure 9. *Neurons respond favorably to imposed tension.* (A) Sample image of intact proximal stump subject to 20% loading, from which axon number and density are calculated. Bar: 500µm. (B) Sample image of proximal neurons from which axonal geometry is calculated. Bar: 10µm. (C-D) Sample laminin staining indicates compaction of basal lamina 3 weeks after nerve severing. Bars: 10µm (E-G) Axonal diameter decreases, and axon number and density increase with stretch. * significantly different from 0%, strain, $p<0.05$; § significantly different from 10% strain, $p<0.05$.

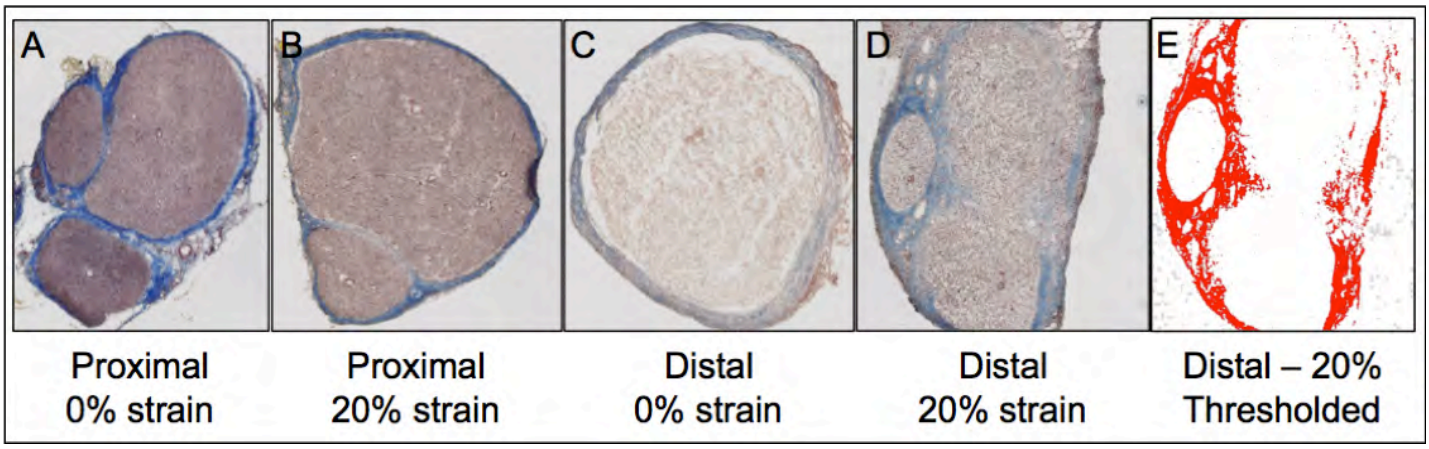

Figure 10: *Connective tissue is destabilized in degenerating distal, but not proximal nerve stumps.* Trichrome staining indicates a pronounced epineurial border (blue labeling, A-B) in both unstretched and stretched proximal stumps, but lack of a defined epineurial border in unstretched and stretched distal stumps (C-D) after 21 days. A loss of structural integrity within the borders of the epineurium is also evident. Colorimetric thresholding using Otsu's method indicates spread of diffuse connective tissue beyond original epineurium.

Cumulatively, these studies have convincingly and demonstrated the feasibility and utility of the proposed approach, and provide compelling differences in nerve morphology, both with and without imposed tension, at early time points. These studies have also provided additional design criteria for the next generation of the device, which we propose to use in long-term survival studies upon securing new sources for funding.

KEY RESEARCH ACCOMPLISHMENTS

- Design and fabrication of two novel biomedical devices for lengthening peripheral nerves in vivo, as a strategy for accelerating nerve regeneration.
- Successful implantation and usage of devices in a rat sciatic nerve injury model for up to six weeks, quantitative assessment of neural regeneration over a 3-week period, and qualitative observation of successful neural regeneration over a 6-week period.
- Discovery that an absence of tension does not result in appreciable organelle accumulation or cytoskeletal degradation.
- Discovery that mechanical loading does not adversely affect the outgrowth of regenerating axons, based on axon density, axon number, and general tissue morphology.
- Discovery that mechanical loading provides, at minimum a 4 mm (~33% for a 12mm defect) head start to regeneration compared to traditional no-tension regenerative strategies.

REPORTABLE OUTCOMES

- *Conference abstract:* Wilson, R., Fisher, J.P., Shah, S.B. (2010) "Peripheral Nerve Regeneration Using a Tension-inducing Scaffold." BMES 2010 Annual Meeting, Austin, Texas.
- *Conference abstract:* Chuang, T.-H., Wilson, R., Fisher, J.P., Shah, S.B. (2011) "A Novel Internal Fixator Device for Peripheral Nerve Regeneration." BMES 2011 Annual Meeting, Hartford, Connecticut.
- *Publication:* Chuang, T.-H., Wilson, R., Fisher, J.P., Shah, S.B. (2011) "A novel biomedical device for tensile loading of peripheral nerves to promote regeneration." Tissue Engineering C. 19(6):427-437.
- *Invention disclosure submitted:* Chuang, T.-H., Wilson, R., Fisher, J.P., Shah, S.B. (2011) "A biomedical device for securing and stretching peripheral nerves." *(submitted to University of Maryland, College Park OTC and UCSD Tech Transfer office concurrent with manuscript acceptance.)*

CONCLUSION

Most strategies for transected peripheral nerve repair focus on bridging the gap in a tension-free setting. The role of a biomechanical stimulus has not been broadly explored. We present a novel biomedical device that is able to impose tensile loading to severed nerve stumps towards the acceleration of peripheral nerve regeneration. The primary innovation of our multi-disciplinary proposal lies in the integration of tensile loading (stretch) and tissue engineering strategies for peripheral nerve regeneration. By imposing tensile loads in parallel with existing tissue engineering strategies for nerve repair (e.g., a nerve guidance channel), we anticipate significantly accelerated nerve regeneration. Progress to date has demonstrated the feasibility of such a strategy, a lack of any adverse effects of upto 20% tension, and early promising regenerative outcomes, providing us confidence for executing and interpreting in vivo studies in future studies.

REFERENCES

1. Covey, D.C. (2006). Combat orthopaedics: a view from the trenches. J Am Acad Orthop Surg *14*, S10-17.
2. Hofmeister, E.P., Mazurek, M., and Ingari, J. (2007). Injuries sustained to the upper extremity due to modern warfare and the evolution of care. J Hand Surg Am *32*, 1141-1147.
3. Schmidt, C.E., and Leach, J.B. (2003). Neural tissue engineering: strategies for repair and regeneration. Annu Rev Biomed Eng *5*, 293-347.
4. Abe, I., Ochiai, N., Ichimura, H., Tsujino, A., Sun, J., and Hara, Y. (2004). Internodes can nearly double in length with gradual elongation of the adult rat sciatic nerve. J Orthop Res *22*, 571-577.
5. Bray, D. (1984). Axonal growth in response to experimentally applied mechanical tension. Dev Biol *102*, 379-389.
6. Bueno, F.R., and Shah, S.B. (2008). Implications of tensile loading for the tissue engineering of nerves. Tissue Eng Part B Rev *14*, 219-233.
7. Pfister, B.J., Iwata, A., Meaney, D.F., and Smith, D.H. (2004). Extreme stretch growth of integrated axons. J Neurosci *24*, 7978-7983.
8. Topp, K.S., and Boyd, B.S. (2006). Structure and biomechanics of peripheral nerves: nerve responses to physical stresses and implications for physical therapist practice. Phys Ther *86*, 92-109.
9. Zheng, J., Lamoureux, P., Santiago, V., Dennerll, T., Buxbaum, R.E., and Heidemann, S.R. (1991). Tensile regulation of axonal elongation and initiation. J Neurosci *11*, 1117-1125.
10. Oh, S.H., Kim, J.H., Song, K.S., Jeon, B.H., Yoon, J.H., Seo, T.B., Namgung, U., Lee, I.W., and Lee, J.H. (2008). Peripheral nerve regeneration within an asymmetrically porous PLGA/Pluronic F127 nerve guide conduit. Biomaterials *29*, 1601-1609.
11. Oh, S.H., and Lee, J.H. (2007). Fabrication and characterization of hydrophilized porous PLGA nerve guide conduits by a modified immersion precipitation method. J Biomed Mater Res A *80*, 530-538.

APPENDICES

Appended is a reprint of our publication. It provides additional details on methodology and key results in support of milestones achieved.

TISSUE ENGINEERING: Part C
Volume 19, Number 6, 2013

DOI: 10.1089/ten.tec.2012.0021

Methods Article

A Novel Internal Fixator Device for Peripheral Nerve Regeneration

Ting-Hsien Chuang, PhD,[1,2,*] Robin E. Wilson, BS,[3,*] James M. Love, BS,[1] John P. Fisher, PhD,[1] and Sameer B. Shah, PhD[1,2]

Recovery from peripheral nerve damage, especially for a transected nerve, is rarely complete, resulting in impaired motor function, sensory loss, and chronic pain with inappropriate autonomic responses that seriously impair quality of life. In consequence, strategies for enhancing peripheral nerve repair are of high clinical importance. Tension is a key determinant of neuronal growth and function. *In vitro* and *in vivo* experiments have shown that moderate levels of imposed tension (strain) can encourage axonal outgrowth; however, few strategies of peripheral nerve repair emphasize the mechanical environment of the injured nerve. Toward the development of more effective nerve regeneration strategies, we demonstrate the design, fabrication, and implementation of a novel, modular nerve-lengthening device, which allows the imposition of moderate tensile loads in parallel with existing scaffold-based tissue engineering strategies for nerve repair. This concept would enable nerve regeneration in two superposed regimes of nerve extension—traditional extension through axonal outgrowth into a scaffold and extension in intact regions of the proximal nerve, such as that occurring during growth or limb-lengthening. Self-sizing silicone nerve cuffs were fabricated to grip nerve stumps without slippage, and nerves were deformed by actuating a telescoping internal fixator. Poly(lactic co-glycolic) acid (PLGA) constructs mounted on the telescoping rods were apposed to the nerve stumps to guide axonal outgrowth. Neuronal cells were exposed to PLGA using direct contact and extract methods, and they exhibited no signs of cytotoxic effects in terms of cell morphology and viability. We confirmed the feasibility of implanting and actuating our device within a sciatic nerve gap and observed axonal outgrowth following device implantation. The successful fabrication and implementation of our device provides a novel method for examining mechanical influences on nerve regeneration.

Introduction

Peripheral nerve injury may result from trauma, cancer, or congenital defects,[1–3] with the severity of injury categorized by the degree and reversibility of structural changes to the nerve.[4,5] Recovery from peripheral nerve damage, especially for a transected nerve, is rarely complete, resulting in impaired motor function, sensory loss, and chronic pain with inappropriate autonomic responses that may seriously impair quality of life. It is estimated that more than 50,000 peripheral nerve repair procedures are annually performed in the United States alone, imposing a financial burden of 7 billion dollars per year.[2] In consequence, strategies for enhancing peripheral nerve repair are of high clinical importance.

Short gaps (<10 mm) may be readily bridged by surgical reconnection of stumps[6] or through a variety of autologous and nonautologous nerve guidance channels (NGCs).[3,7–14] Autologous nerve grafts remain the gold standard for repairing longer nerve gaps, but are in limited supply, exhibit donor site morbidity, and may exhibit a size mismatch compared to the transected nerve. Nonautologous grafts can incorporate biological or synthetic components and have been designed with increasing complexity. Biological grafts include acellular nerve grafts or use skeletal muscle,[15,16] vein[17–19], and tendon,[20] while synthetic NGCs have been fabricated with a variety of geometries, porosities, and material properties.[3,21] Grafts have also been designed to incorporate chemical and biological cues to encourage nerve regeneration, such as Schwann cells, stem cells, or neurotrophic factors.[22–25] Despite such developments, engineered NGCs do not perform as well as autografts, particularly for large defect sizes, when degeneration is more likely to outpace neuronal extension.[26] Therefore, there is still a need to develop a strategy for repairing large gaps (>10 mm).

Tensile loading is an influence on nerve growth and function that has been underutilized in the context of nerve

[1]Fischell Department of Bioengineering, University of Maryland, College Park, Maryland.
[2]Departments of Orthopedic Surgery and Bioengineering, University of California, San Diego, La Jolla, California.
[3]Department of Biomedical Engineering, Case Western Reserve University, Cleveland, Ohio.
*These two authors equally contributed to this work.

regeneration. Nerves bear tension under several physiological scenarios. Peripheral nerves exist under tension, releasing strains of up to 11% following transection,[27–29] and may deform additionally, in some cases upward of 20%, during joint movement.[30–32] During growth, axonal tension serves as a survival and stabilization signal for axons. Conversely, neurites under no tension retract.[33] It has also been shown that moderate tensile loads can accelerate neuronal growth, both *in vitro* and *in vivo*.[34–39]

Toward the development of more effective nerve regeneration strategies, in this study, we detail the design, fabrication, and preliminary implementation of a novel internal fixator device. This modular device, by imposing mechanical loads on regenerating nerves in parallel with existing tissue engineering strategies for nerve repair, facilitates two regimes of nerve extension—traditional extension through axonal outgrowth into an engineered scaffold and novel extension of intact regions of the proximal nerve (Fig. 1a).

Materials and Methods

Animals

We used adult 14-week-old male Sprague-Dawley rats (350–400 g), based on the use of this strain in a number of nerve regeneration studies and its well-characterized sciatic nerve architecture.[40, 41] Animal use protocols were approved by the UMCP and UCSD Institutional Animal Care and Use Committees.

Device fabrication

The device is composed of three major components: self-sizing silicone spiral nerve cuffs, poly(lactic co-glycolic) acid (PLGA) NGCs, and a mechanical backbone to which the cuffs and NGCs are attached. Dimensions for the device used with rat sciatic nerves are provided in Figure 1b.

Spiral nerve cuffs. To impose tensile loading on the transected nerve, self-sizing spiral nerve cuffs were created to firmly grip the proximal and distal nerve stumps, without exerting excessive compression. We modified a protocol for the fabrication of spiral cuff electrodes[42]; however, no electrode was embedded in our cuffs (Fig. 2a). Two Silastic® silicone sheets (Dow Corning) of 0.005 inches in thickness were bound together using a silicone adhesive (biomedical grade Silastic® elastomer MDX4-4210; Dow Corning). The first sheet was unstretched, and placed adjacent to one stainless steel slab. The second sheet was stretched to a specified strain (50%, 60%, 70%, or 100% strain; cf. Fig. 2d), and attached to a second grooved slab via an additional layer of silicone adhesive, to create a textured surface on the interior surface of the cuff that would increase friction between the cuff and nerve stump. The sandwiched silicone composite was cured at 60°C for 2 h. After curing, the resultant spiral sheet was cut to a length of 0.5 cm, to enable self-sizing of approximately one and a quarter spirals around the sciatic nerve of adult male Sprague-Dawley rats (350–400 g).

Nerve guidance channel. Nerve guides were prepared using a modified phase inversion technique.[43] PLGA (lactic to glycolic acid mol ratio of 75:25, M_w = 66,000–107,000; Sigma) was dissolved in tetraglycol (Sigma) at 60°C (10 wt%) and then Pluronic® F-127 was added (3 wt%) to increase the hydrophilicity. Alginate hydrogel rods were formed by first dissolving alginate (Sigma) in water (4 wt%) and injecting the solution into 2% $CaCl_2$ with a syringe (14-gauge needle). After saturation, the alginate hydrogel was immersed in the PLGA/Pluronic F-127 solution. Due to phase separation between polymer (PLGA/F127) and nonsolvent (water in alginate hydrogel), PLGA precipitated onto the alginate rod as water diffused out of the hydrogel. The construct was thoroughly washed in water for 24 h to remove excess tetraglycol. After retrieval of the alginate rod; the resultant

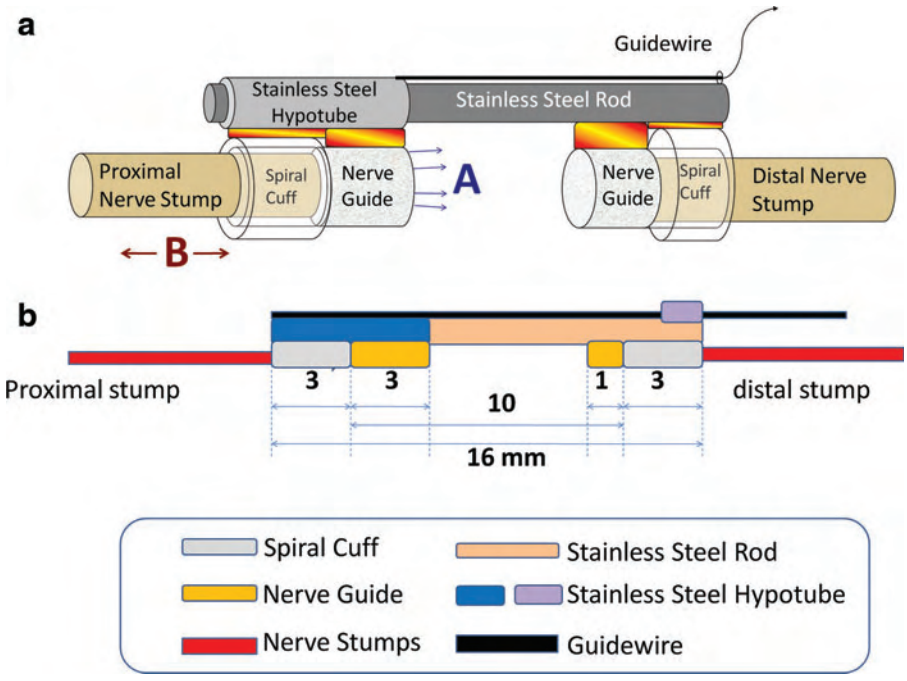

FIG. 1. Device design. The nerve stretching device is composed of spiral nerve cuffs, poly(lactic co-glycolic) acid (PLGA) nerve guidance channel (NGC), and stainless steel backbone **(a)** Two regions of regeneration, A: Enhanced axonal outgrowth into a tissue engineered nerve guide/scaffold; B: Lengthening of intact regions of nerve stumps–cf. limb lengthening. **(b)** Dimensions of the device. Color images available online at www.liebertpub.com/tec

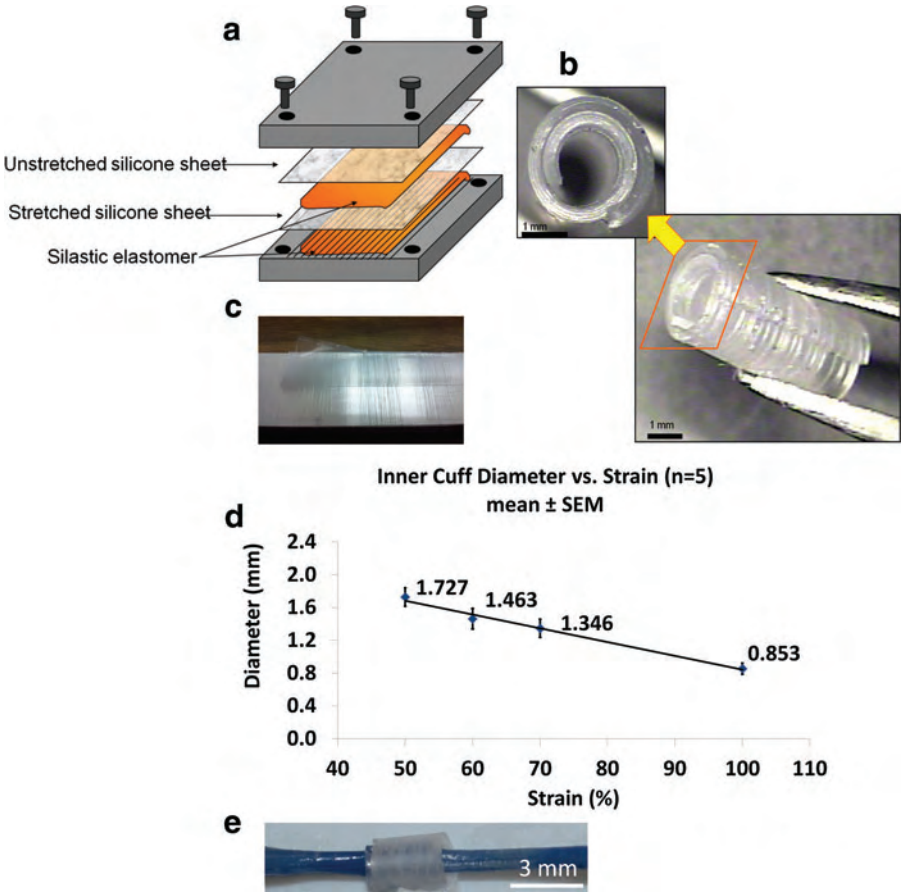

FIG. 2. Fabrication and characterization of spiral nerve cuff. **(a)** Two layers of silicone sheets (with one being stretched) are glued together; **(c)** the microgroove pattern on the slab is transferred to the cuff; **(b)** the resultant curled nerve cuff after curing; **(d)** inner diameter decreases with increasing % strain of prestretched silicone sheet; **(e)** sample *ex vivo* testing of trypan blue-labeled nerve in cuff revealed no appreciable compression or tethering. Color images available online at www.liebertpub.com/tec

PLGA tubes were dried at room temperature and cut to the desired length.

Mechanical backbone. A stainless steel rod of 1.57 mm in diameter (Component Supply Co.) was used as the backbone of the device. This material was selected due to its strength and previous applications in implanted devices. The end of the device to be affixed to the proximal stump consisted of one spiral nerve cuff and a PLGA NGC fixed onto a 14-gauge thin wall stainless steel hypotube (Component Supply Co.), designed to slide along the stainless steel rod. The hypotube had a 28-gauge guidewire attached, enabling us to stretch the proximal nerve stump. A second spiral nerve cuff and PLGA NGC were fixed to the distal terminal of the inner stainless steel rod. Medical grade n-butyl cyanoacrylate adhesive was used to affix the cuffs, guidance channel, and guidewire to the device backbone.

Device characterization

Spiral nerve cuffs. To find the correlation between preloaded strain in the silicone sheet and degree of spiral curl, the inner diameters of nerve cuffs of 50%, 60%, 70%, and 100% strains were measured and compared. Inner diameter was defined as the distance from the inner most tip of the curved cuff to the surface 180° from this starting point. We examined the capability of cuffs to grip nerves without slippage in rat cadavers ($n=6$) and *in vivo* ($n=8$). We exposed rat sciatic nerves and then deployed self-sizing spiral nerve cuffs (fabricated under 100% strain, Fig. 2d.) by unwinding them and letting them roll onto the nerves. The inner edge was gently pulled with forceps to ensure that there was no gap between cuff and nerve. In cadavers, we actuated the device the entire possible 6 mm (Fig. 1b). *In vivo*, we stretched nerves 20% beyond physiological strain (~2 mm), and examined cuff positioning between 1 day and 3 weeks later.

We also assessed the possibility of nerve compression by the cuffs. During device implantations *in situ* and *in vivo*, the interface of the nerve and cuff was examined at 5× –20× magnification, to confirm that the nerve did not narrow upon entry to the cuff, indicated by a change in the diameter or trajectory of the nerve at the nerve–cuff interface. These effects were quantified *ex vivo*. We wrapped cuffs around nerves soaked in trypan blue ($n=4$), which provided contrast between nerve and cuff. Digital images (three images/nerve, from three different angles/nerve) were captured to compare nerve geometry at the nerve–cuff interface and away from the cuff. We first compared the angular trajectory of the nerve 0 mm (nerve-cuff border) to 0.25 mm from the cuff with the trajectory of the nerve in the adjacent nerve segment 0.25–0.5 mm from the cuff. In addition, the nerve diameter at the cuff–nerve interface (0 mm) was compared to the diameter 0.5 mm away from the cuff. Control trajectories and diameters were measured >3 mm from the cuff; angular trajectories in adjacent 0.25 mm

segments and diameters flanking these segments were compared. A difference in the ratio of trajectories in adjacent regions, coupled with a difference in diameter, would suggest compression or tethering.

PLGA cytotoxicity. Both direct contact and test on extract methods of *in vitro* cytotoxicity testing were performed on the SH-SY5Y neuronal (neuroblastoma) cell line (ATCC # CRL-2266). The impact of leachable factors from PLGA on cell viability was performed as suggested in the ISO 10993-5 standard. Cell culture medium (90% MEM/F12, 10% fetal bovine serum) was incubated in PLGA-coated Petri dishes at 37°C for 24 h and then was used to feed SH-SY5Y cells. To test the effects of PLGA on cell growth, after 96 h of culture SH-SY5Y cells were collected by trypsinization of adherent cells. The numbers of total cells were estimated by cell counting using hemocytometer and statistically compared by Student's *t*-test (type I error $\alpha = 0.05$). Cell viability was tested using Live/Dead© fluorescence assay. Morphology of cells fed with PLGA-incubated medium was observed under an inverted light microscope. For the direct contact study, visualization of morphology of cells grown on PLGA using traditional transmitted light microscopy was difficult due to the opaque nature of the thick PLGA layer. Therefore, SH-SY5Y cells were first seeded onto discs coated with PLGA or PLGA followed by laminin in a Petri dish filled with culture medium. Discs were then inverted onto coverslips for imaging. For identifying the contours of the neuronal cells, they were stained with Alexa Fluor® 488 conjugated wheat germ agglutinin, which binds to sialic acid and N-acetylglucosaminyl sugar residues that reside on the cell membrane.[44] Subsequent imaging was performed on an inverted widefield fluorescence microscope (Nikon TE-2000U) using filters appropriate for FITC visualization and a Leica SP5 confocal imaging system and a 63× objective at a resolution of 0.4805 μm/pix. For the latter, an argon laser enabled excitation at 488 nm and emission was captured between 500 and 550 nm.

Device implantation

Implantations were initially performed in cadavers, and then *in vivo*. For initial *in situ* studies, 14-week-old adult male Sprague-Dawley rats were sacrificed by CO_2 euthanization. For *in vivo* studies, 14-week-old adult male Sprague-Dawley rats were anesthetized using 5% isoflurane inhalation anesthesia, followed by injection of analgesic (0.05 mg/kg buprenorphine) and antibiotics (5 mg/kg Baytril®). Anesthesia was maintained by 2% isoflurane inhalation all through the surgery. The surgical site was shaved and sterilized, and the sciatic nerve was exposed and severed as above. The device was implanted; the incision to the muscle was closed by 4-0 Vicryl® suture and the incision to the skin with 3-0 Prolene® monofilament suture. The rat was kept for up to 3 weeks with full access to food and water.

The sciatic nerve was exposed by separating branches of the hamstring muscles. A 10 mm segment of sciatic nerve proximal to the trifurcation was removed, and then the device was implanted. The backbone was oriented along the original axis of the nerve within the nerve bed. Proximal and distal nerve stumps were wrapped with the spiral nerve cuffs. Forceps were used to carefully grasp the epineurial sheath, and bring the tip of the nerve stump toward the open ends of the PLGA NGC. No more than 0.25 mm of the nerve was placed within the channel, to ensure guidance within the channel. The guidewire was then pulled to stretch the proximal stump of the sciatic nerve proximal stump to the desired length. Once the device was positioned appropriately, it was prevented from translating by fixing it to the underlying muscle bed with stainless steel anchors (28 gauge). A group of rats also underwent the same surgical protocol without device implantation. Contralateral nerves were harvested as controls.

Characterization of response to device

Following sacrifice, a gross assessment of device tolerance and immunohistochemistry were performed. The length of regenerating proximal nerve stump that extended beyond the cuff was measured and then rapidly frozen down in chilled isopentane for histology preparation. The regenerating nerve was embedded in Optimal Cutting Temperature (Sakura Fintek USA, Inc.) and cut into 10-μm sections for immunostaining. Primary antibodies including mouse anti-rat SMI-31 monoclonal antibody (Covance) diluted at 1:200 and rabbit anti-rat S-100 polyclonal antibody (Sigma-Aldrich) diluted at 1:200 along with secondary antibodies goat anti-mouse Alexa-Flour 488 conjugated and goat anti-rabbit Alexa-Flour 594 conjugated diluted at 1:200 (Invitrogen) were used and then visualized with confocol microscopy as above (Leica SP5), using filters appropriate for Texas Red visualization.

Results

Spiral nerve cuffs

Spiral nerve cuffs were successfully fabricated, and the microgroove pattern was successfully transferred to the inner surface of the cuff (Fig. 2b, c). Measurements of the inner diameter of the spiral nerve cuffs showed a decreasing trend of inner diameter with increasing strain in the stretched silicone sheet (Fig. 2d). Pilot testing of the efficacy of nerve gripping indicated that cuffs of 70% and 100% preloaded strain (average inner diameter of 1.35 and 0.85 mm, respectively) successfully held the nerve without slippage. We elected to use the 100% cuff for further characterization, as self-sizing was more consistent. For 14 out of 14 tests (100%) in cadavers and *in vivo*, there was no indication that nerves detached from the cuffs, or slid within the cuff, based on comparison of cuff position to reference marks at the proximal cuff–nerve boundary. The inner surface of spiral nerve cuff was in close contact with the nerve stump but caused minimal nerve compression. In all *in situ* and *in vivo* experiments ($n = 14$), the trajectory and diameter of the nerve outside of the cuff was compared to its trajectory entering the cuff, and no indication of compression or tethering was observed in 100% (14/14) of these qualitative assessments. This was tested more formally *ex vivo*, by quantifying the geometry and trajectories of nerves entering the cuffs. Nerves were dyed with trypan blue, to enhance contrast with the optically clear cuff. Consistent with qualitative observations of a continuous nerve trajectory into the cuff (e.g., Fig. 2e), based on the ratio of trajectories and diameters in adjacent regions at and away from the cuff (control), no deviation in trajectory

(control: 1.00 ± 0.002 vs. cuff: 1.00 ± 0.006, $p = 0.41$, $n = 8$ interfaces) or diameter (control: 0.99 ± 0.01 vs. cuff: 0.98 ± 0.01, $p = 0.67$, $n = 8$ interfaces) was observed at the interface of cuff entry.

PLGA nerve guidance channel

Due to phase separation, white solid state PLGA gradually precipitated onto the water-eluding alginate hydrogel. After retrieval of the alginate rod, a hollow PLGA tube was produced (Fig. 3a). The PLGA tube was then cut into small segments to serve as NGCs (Fig. 3b). Cross-sectional scanning electron microscopy images showed that the PLGA tubes had a porous structure (Fig. 3c) as reported previously.[45]

PLGA cytotoxicity

SH-SY5Y cell fed with medium preincubated with PLGA showed similar morphology (Fig. 4b) to that of control (Fig. 4a). Live/Dead® cell viability assay also showed that only very few dead cells were present (Fig. 4d; 4c as control). Quantification revealed no significant difference in viability between treated and control cells ($94\% \pm 3.71\%$ vs. $98\% \pm 0.27\%$ (mean ± standard error of the mean), respectively; $p = 0.30$; Student's *t*-test, $n = 3$). Thus, both morphologically and biochemically, no signs of cytotoxicity were observed. For the effects of PLGA on cell division and growth, the experimental group displayed no significant difference compared with the control group (Fig. 4e). For direct observation of morphology of cells grown on PLGA, cell membranes were labeled with fluorescent wheat germ agglutinin. Confocal imaging revealed that SH-SY5Y cells adhered to a laminin-coated PLGA substrate, spread, and extended outward (Fig. 4f). Outgrowth and cell density on a laminin-coated surface was superior to that on PLGA alone (data not shown).

In situ *implantation—feasibility of no-slip actuation*

The assembled device is shown *ex vivo* under nonactuated and actuated configurations (Fig. 5a, b). Deployment of the device was first performed in a rat cadaver, to demonstrate the feasibility of actuation. The device was implanted within a nerve defect, with the nerve stumps wrapped by spiral cuffs (Fig. 5c). By pulling the guidewire attached to the hypotube sliding over the rod, the nerve stump of proximal end was successfully stretched and placed under tension (Fig. 5d). This configuration corresponds to the maximum possible one-time deformation (6 mm) of the nerve, which is limited by guidance channel dimensions. Though unlikely to be physiologically relevant, this cadaver experiment demonstrates no-slip gripping of nerve at substantial deformation, and thus opposing tension.

In vivo *implantation—feasibility of promoting regeneration*

The device was successfully deployed across a sciatic nerve defect in anesthetized rats (Fig. 6a), and tensioned to physiological (~10%; $n = 4$) or super-physiological deformation (~20%; $n = 4$), demonstrating feasibility of device implantation and actuation *in vivo*. While a comparative, quantitative assessment of regeneration is underway, but outside of the scope of this study, several observations confirmed the feasibility of using our device to probe regeneration. All animals tolerated the device for up to 3 weeks without obvious signs of infection. Upon reopening the incision, as expected, fibrotic encapsulation of the device was observed (Fig. 6b). Nevertheless, the device was cleanly excised, with minimal connective tissue bound to either the stainless steel backbone (Fig. 6c) or the attached cuff/nerve complex (Fig. 6d). Moreover, both nerve stumps remained confined within the cuffs without apparent slippage, and the proximal stump extended about 6 mm beyond the cuff into the guidance channel (Fig 6d; guidance channel removed to visualize nerve). Nerve confinement and alignment by the device was in sharp contrast to injured nerves allowed to recover for 1 week in the absence of a guidance channel, which were misaligned and blocked from regeneration by fibrosis (Fig. 6e, f).

Immunolabeling indicated the presence of axons in the regenerated region of the stump, indicated by positive

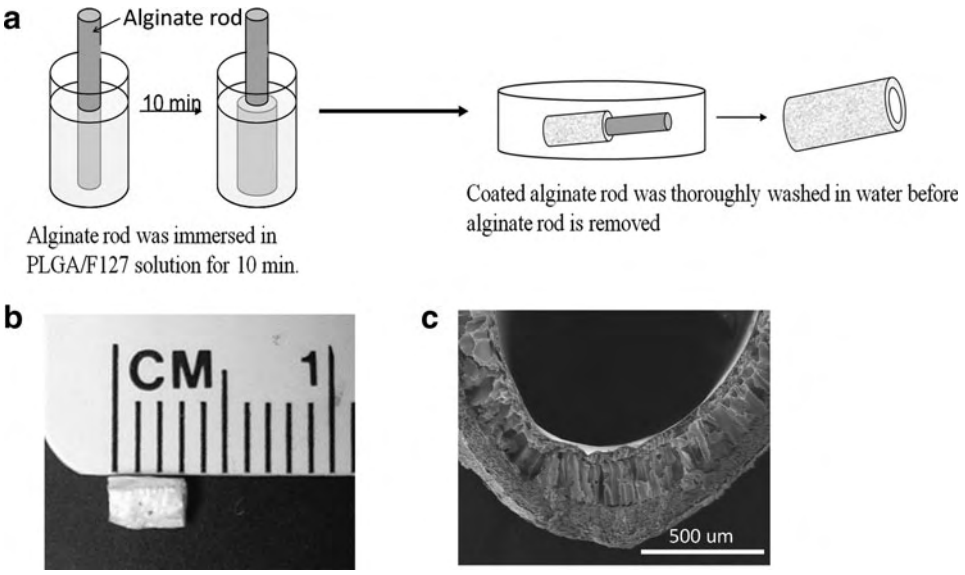

FIG. 3. Fabrication of PLGA NGC. **(a)** Alginate rod was immersed in PLGA/Pluronic F-127 solution for 10 min. Tubular PLGA layer is formed due to phase separation when water diffuses out the alginate rod; coated alginate rod was thoroughly washed in water before alginate rod is removed **(b)** PLGA tube is cut into short segments to serve as NGC. **(c)** Cross section scanning electron microscopy picture of PLGA tube.

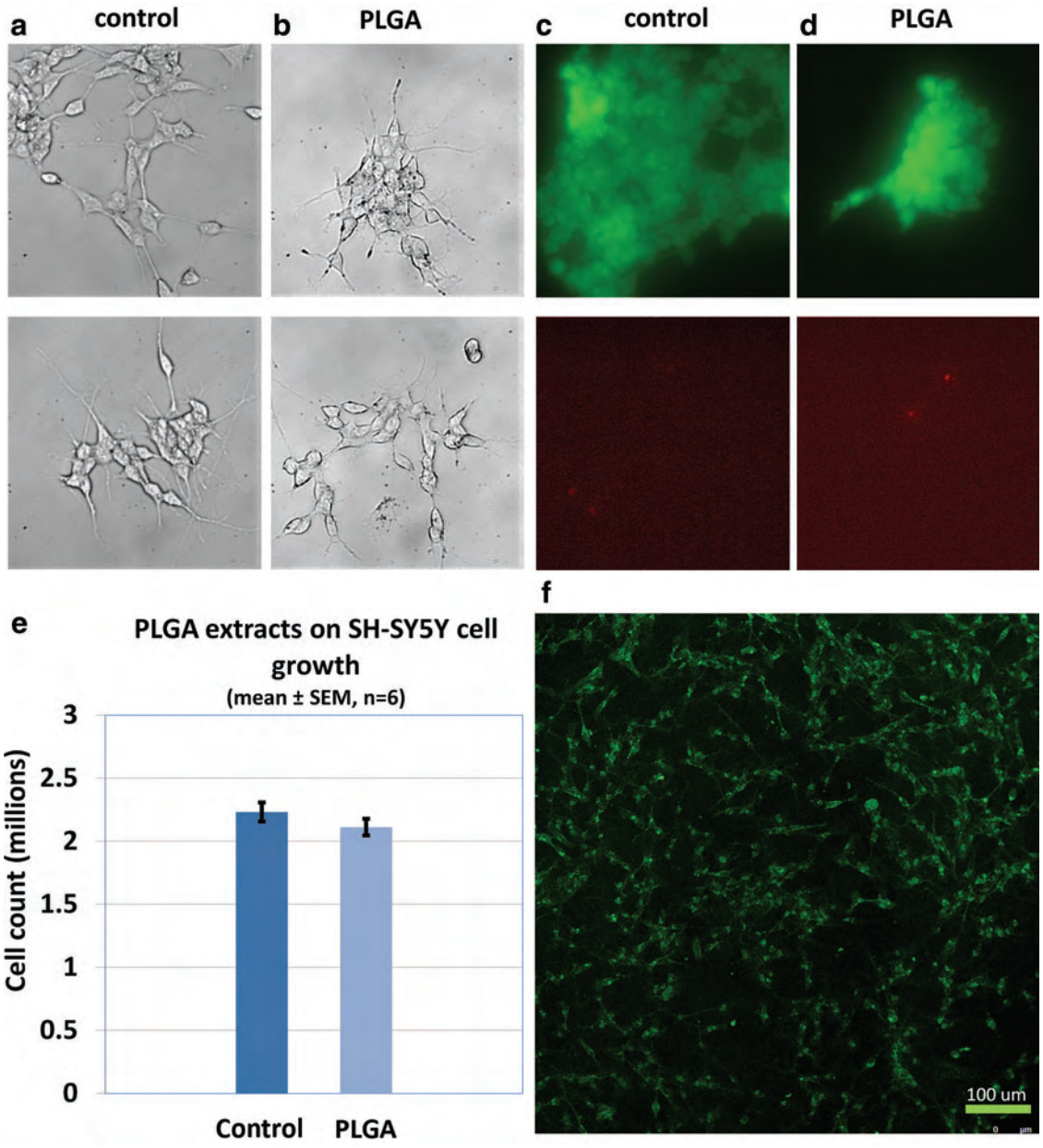

FIG. 4. PLGA cytotoxicity. **(a–d)** Cells were fed with PLGA-incubated culture medium to test whether leachable substances from a PLGA scaffold would have cytotoxic effects on the cells. **(a, b)** No signs of PLGA cytotoxicity was observed in terms of cell morphology; **(c, d)** Live/Dead® cell viability assay indicated very few dead cells; **(e)** No statistical difference was found between control and PLGA group, $p = 0.05$. **(f)** Visualization of morphology of cells grown on PLGA by fluorescent wheat germ agglutinin staining of cell membranes. SH-SY5Y cells attached, spread, and proliferated on PLGA. Color images available online at www.liebertpub.com/tec

staining of phosphorylated neurofilaments (SMI31 antibody) (Fig. 7b, c) and Schwann cell marker (S100 antibody) (Fig. 7e, f). The parallel alignment of axons and Schwann cells was similar to that of contralateral controls (Fig. 7d, g). Collectively, these preliminary *in vivo* data indicated the feasibility of device usage *in vivo*, and provide confidence in the deployment of such devices to test hypotheses regarding the role of tensile loading in nerve regeneration.

Discussion

Toward the implementation of a novel strategy for accelerating peripheral nerve regeneration, we have successfully designed, fabricated, and implanted across a rat sciatic nerve gap a modular device that enables simultaneous lengthening of the proximal nerve stump and axonal outgrowth into an engineered scaffold. The novelty of our approach lies in the application of tensile loading (stretch) as a strategy to accelerate peripheral nerve regeneration, and the seamless integration of this strategy with existing tissue engineering strategies for nerve repair.

A role for tension in nerve repair

Although several recent studies implicate tension as a key regulator of neuronal survival, the role of tension in

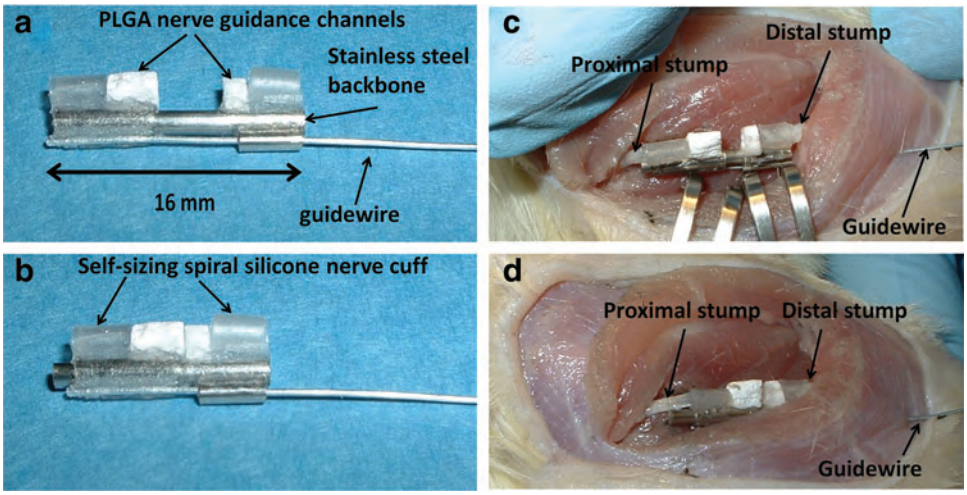

FIG. 5. Demonstration of slip-free nerve deformation. **(a, b)** Device fully extended and maximally actuated, *ex vivo*. **(c, d)** Fully extended device and actuated device in a rat sciatic nerve defect. Note that implanted device can stretch the nerve stumps 6 mm without slippage. Color images available online at www.liebertpub.com/tec

peripheral nerve repair is debatable. In clinical practice, tension-free repair remains the preferred treatment.[46,47] This is motivated by suggestions that excessive tension results in scar tissue formation and adhesion[48,49] or impairs blood supply[50,51]; studies showed blood flow reduced ~50% when nerves are stretched to 10%.[52,53] On the other hand, Sunderland *et al.* showed that modest levels of tension were well tolerated in rat sciatic nerve regeneration model,[54] and robust nerve regeneration was observed at 4 weeks in all except the 9 mm-repair group. Moreover, Smith *et al.* demonstrated the capacity of integrated axons to undergo substantial growth via continuous mechanical tension; indeed a stretch-induced axonal growth of 1 cm in length by 10 days of stretch was achieved.[55] The most compelling evidence for a role of tension in nerve regeneration may be found in animal and human models of limb lengthening, where nerves tolerate substantial deformations during the lengthening process.[34,56–65]

Therefore, the more appropriate debate should be on defining an appropriate threshold beyond which tension is detrimental. Our device design is motivated by the hypothesis that maintaining physiological strain during the lengthening process will accelerate nerve regeneration.

Novel device features and characterization

Our device consisted of three key design features: silicone spiral nerve cuffs to hold the nerve, a telescoping stainless steel backbone to enable nerve deformation, and PLGA NGCs to promote axonal outgrowth.

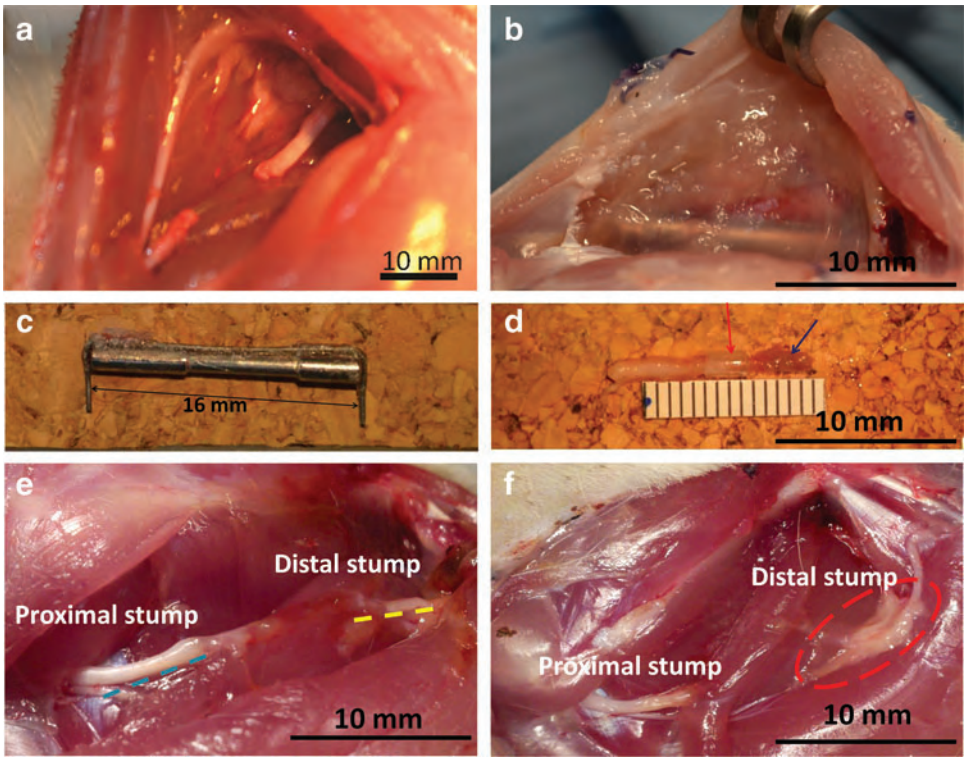

FIG. 6. Response to 2-week implantation of device. **(a)** A nerve gap was created by removal of 10 mm segment from the rat sciatic nerve. **(b)** Following 2 weeks of implantation, minor fibrosis was observed at the implantation site. **(c)** The stainless steel backbone was cleanly extracted at 2 weeks. **(d)** The proximal stump was still securely held by the nerve cuff (red arrow), and the regenerating tip extended beyond the cuff ~6 mm (blue arrow). **(e, f)** In the absence of device implantation the two stumps remained disconnected and misaligned. A bulge was observed at the proximal stump and the degenerating distal stump appeared fused with surrounding fatty/connective tissue. Color images available online at www.liebertpub.com/tec

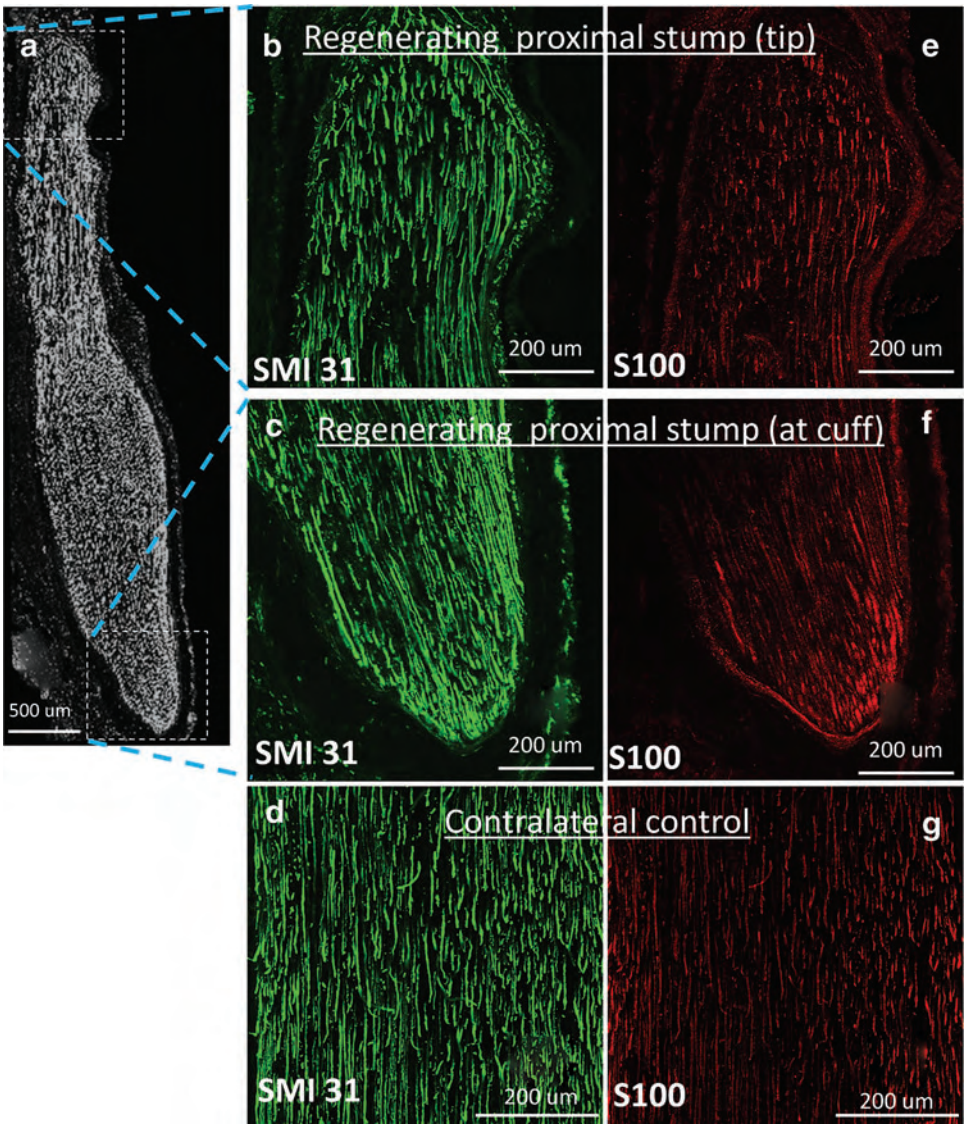

FIG. 7. Evidence of regenerative neural outgrowth. **(a)** The regenerating nerve extended ~6 mm beyond the cuff, and was stained with anti-SMI-31 **(a–c)** and anti-S100 **(e, f)** antibodies, which labeled phosphorylated neurofilaments and Schwann cells, respectively. **(d, g)** The contralateral sciatic nerve was stained with the same two markers and served as a control. Color images available online at www.liebertpub.com/tec

Self-sizing spiral cuffs, modeled after spiral cuff electrodes,[42] were fabricated to a desired inner diameter (Fig. 2d). They were also patterned with microgrooves on the inner surface to increase friction between the cuff and underlying nerve. Self-sizing cuffs successfully held nerves during deformation without excessive compression (Fig. 2e). In contrast to sutures, which would concentrate stresses in their vicinity during stretch, cuffs also promoted the distribution of loads over a larger surface area. Mounting the cuffs on telescoping rods enabled actuation through a simple guidewire, intracorporeally. While there is room for innovation in controlling the degree of actuation, the fact that the guidewire is the only piece of the device protruding from the body is attractive, and a significant advantage over an external fixator design.

Though any scaffold may be integrated into our device, we initially selected tubular PLGA/Pluronic F-127 conduits as NGCs. This material was selected based on its hydrophilicity, our ability to carefully control its geometry, even in hydrous conditions, and its promise as a guidance channel.[43] We confirmed that the resultant PLGA nerve guidance had a porous structure (Fig. 3c), which is likely to be permeable to nutrients. We extended the previous fabrication and characterization of PLGA NGCs by performing direct and indirect contact cytotoxicity tests. Though PLGA is a well-established biomaterial, our use of neuronal cells extends previous studies on fibroblasts,[66–68] and is directly relevant to our intended application for neuronal regeneration. For both direct contact and extracts testing, no signs of cytotoxicity were found in terms of cell proliferation and cell viability. With respect to morphology, SH-SY5Y cells on PLGA exhibited adherent cell bodies with projections extending outward, similar to neuronal cells cultured in tissue culture Petri dishes. A substantial improvement in neuronal adherence and neurite morphology was observed when neurons were plated on PLGA coated with laminin. Consequently, this minor, but beneficial change should be incorporated into implanted PLGA NGCs.

Device implantation and surgical implementation

We confirmed the feasibility of implanting our device across a sciatic nerve gap and lengthening the proximal nerve stump without slippage up to 6 mm (~60%) in a rat cadaver

(Fig. 5c, d). This excessive strain would likely be detrimental physiologically, but did confirm the ability to maintain a suture-free grip on a nerve despite considerable opposing tensile loads. Preliminary results *in vivo* were also promising. Nerves were successfully subject to a one-time stretch of ~10% (physiological strain) and ~20% (super physiological strain), and revealed that rats did not show signs of infection, and survived at least 3 weeks before sacrifice. Within this time frame, the proximal nerve stump extended about 6 mm beyond the cuff (Fig. 6d); we further identified regenerating axons as a part of this elongating tissue, based on positive, well aligned labeling of a marker for mature axons, phosphorylated neurofilaments (Fig. 7). Such regenerative growth was in contrast to nerve outgrowth in the absence of intervention, which appeared misaligned, and plagued by interactions with surrounding fatty and connective tissue (Fig 6e, f). These observations indicate the necessity of both NGC and an aligning backbone, to increase the probability of successfully reconnecting nerve stumps.

In practice, because the proximal and distal guidance channels will collide following sufficient lengthening (6 mm total, for our described prototype), an ideal scenario will be to have the channels meet shortly before axons exit the proximal channel. Based on literature values, dimensions of the prototype device assume lengthening over 5–6 days, at conservative lengthening rates of 1 mm/day and axonal outgrowth rates of 0.3 mm/day. However, these rates will eventually be optimized based on empirically determined thresholds for lengthening and axonal outgrowth rates into the scaffold.

Finally, we would be remiss if we did not point out some potential pitfalls of implanting our device *in vivo*. Most anticipated issues are likely to arise due to inflammatory and fibrotic processes. These include jamming of the telescoping mechanism of the hypotube and the inner rod owing to fibrous tissue infiltration, cell infiltration into the nerve gap, and scar formation. We speculate that due to actuation frequently, and primarily at early time points, the jamming of the telescoping mechanism is unlikely and fibrosis will be no more of an issue with our device than any other implanted scaffolds or devices, including an external nerve lengthening device.[69–71] We will test the utility of medical grade expanded polytetrafluoroethylene sleeves as a protective sheath surrounding the device. Another potential drawback is possible infection at the site where guidewire extends from the animal's body. Such a scenario would be treated with antibiotics; however, it should be noted that many peripheral nerve devices, including spiral cuff electrodes,[42] have been successfully implanted with leads exiting the body. Therefore, we speculate that this risk is minimal. Finally, to successfully stretch the proximal nerve stump with the device, the mechanical backbone must be secured to a reference position. In our initial study, we have secured the device to the underlying muscle using simple stainless steel anchors. This is less invasive and appears adequate, based on preliminary short-term survival surgeries; however, should complications arise, anchorage to the femur provides a more invasive, but previously validated option.[69–71]

Comparison to other strategies for nerve regeneration

Our lengthening device is intended to be used in parallel with other guidance strategies, including autologous grafts, synthetic grafts, acellular guidance matrices, and seeded matrices. Consequently, a direct comparison between a passive scaffold and the same scaffold incorporated within our device would be most appropriate. For the device introduced in this study, the appropriate comparisons would be an uncoated passive PLGA scaffold[33] and a passive PLGA scaffold coated with laminin. Differential responses between our device and these scaffolds would reflect effects of mechanical extension of intact regions of the proximal nerve superposed on outgrowth into the scaffold (Fig. 1).

To our knowledge, only one other group has directly evaluated tensile loading as a regenerative strategy. The Ochiai group proposed an intriguing series of articles [69–71] that implemented a direct lengthening device to lengthen proximal and distal nerve stumps. Regeneration rates were equal or greater than those observed with an autologous graft, lending strong support to the hypothesis that mechanical loading can be beneficial to outgrowth. However, three key issues detract from the translational viability of this technology. First, based on their proposed design, nerves are readily lengthened, but the device configuration is not amenable to reattachment without additional surgery (i.e., there is nowhere for outgrowing axons to go). Second, because this design requires a complex external fixator mounted within the adjacent femur, more invasive surgery is required. Finally, nerve ends are secured with suture for tensioning; such attachment is likely to impose compression or uneven strain distributions owing to the discrete sites of attachment, again diminishing the likelihood of successful axonal outgrowth. Through the use of an internal fixator and self-sizing cuffs, we believe that our design has accounted for the most pressing of these issues. Though yet at an early stage of development, the successful fabrication and implementation of our device provides considerable enthusiasm for this device and the broader strategy of mechanical influences on nerve regeneration.

Acknowledgments

This research was supported by grant W81XWH1010773 from the U.S. Army Medical Research and Materiel Command and grant CBET1042522 from the National Science Foundation. We also acknowledge helpful discussions with members of the Neuromuscular Bioengineering Laboratory. Scanning electron microscopy image was taken at the University of Maryland Nanoscale Imaging Spectroscopy and Properties Laboratory.

Disclosure Statement

No competing financial interests exist.

References

1. Burnett, M.G., and Zager, E.L. Pathophysiology of peripheral nerve injury: a brief review. Neurosurg Focus **16,** E1, 2004.
2. Evans, G.R. Peripheral nerve injury: a review and approach to tissue engineered constructs. Anat Rec **263,** 396, 2001.
3. Schmidt, C.E., and Leach, J.B. Neural tissue engineering: strategies for repair and regeneration. Annu Rev Biomed Eng **5,** 293, 2003.

4. Seddon, H.J. Three types of nerve injury. Brain **66,** 247, 1943.
5. Sunderland, S. A classification of peripheral nerve injury produced by loss of function. Brain **74,** 491, 1951.
6. Scherman, P., Kanje, M., and Dahlin, L.B. Bridging short nerve defects by direct repair under tension, nerve grafts or longitudinal sutures. Restor Neurol Neurosci **22,** 65, 2004.
7. Dahlin, L., Johansson, F., Lindwall, C., and Kanje, M. Chapter 28: Future perspective in peripheral nerve reconstruction. Int Rev Neurobiol **87,** 507, 2009.
8. Terenghi, G., Wiberg, M., and Kingham, P.J. Chapter 21: Use of stem cells for improving nerve regeneration. Int Rev Neurobiol **87,** 393, 2009.
9. Zacchigna, S., and Giacca, M. Chapter 20: Gene therapy perspectives for nerve repair. Int Rev Neurobiol **87,** 381, 2009.
10. Donat, J.R., and Wisniewski, H.M. The spatio-temporal pattern of Wallerian degeneration in mammalian peripheral nerves. Brain Res **53,** 41, 1973.
11. Atchabahian, A., Genden, E.M., MacKinnon, S.E., Doolabh, V.B., and Hunter, D.A. Regeneration through long nerve grafts in the swine model. Microsurgery **18,** 379, 1998.
12. Millesi, H., Meissl, G., and Berger, A. The interfascicular nerve-grafting of the median and ulnar nerves. J Bone Joint Surg Am **54,** 727, 1972.
13. Strasberg, S.R., Mackinnon, S.E., Genden, E.M., Bain, J.R., Purcell, C.M., Hunter, D.A., and Hay, J.B. Long-segment nerve allograft regeneration in the sheep model: experimental study and review of the literature. J Reconstr Microsurg **12,** 529, 1996.
14. Bora, F.W., Jr., Bednar, J.M., Osterman, A.L., Brown, M.J., and Sumner, A.J. Prosthetic nerve grafts: a resorbable tube as an alternative to autogenous nerve grafting. J Hand Surg Am **12,** 685, 1987.
15. Fawcett, J.W., and Keynes, R.J. Muscle basal lamina: a new graft material for peripheral nerve repair. J Neurosurg **65,** 354, 1986.
16. Gattuso, J.M., Glasby, M.A., Gschmeissner, S.E., and Norris, R.W. A comparison of immediate and delayed repair of peripheral nerves using freeze-thawed autologous skeletal muscle grafts—in the rat. Br J Plast Surg **42,** 306, 1989.
17. Chiu, D.T., Janecka, I., Krizek, T.J., Wolff, M., and Lovelace, R.E. Autogenous vein graft as a conduit for nerve regeneration. Surgery **91,** 226, 1982.
18. Suematsu, N., Atsuta, Y., and Hirayama, T. Vein graft for repair of peripheral nerve gap. J Reconstr Microsurg **4,** 313, 1988.
19. Strauch, B., Ferder, M., Lovelle-Allen, S., Moore, K., Kim, D.J., and Llena, J. Determining the maximal length of a vein conduit used as an interposition graft for nerve regeneration. J Reconstr Microsurg **12,** 521, 1996.
20. Brandt, J., Dahlin, L.B., and Lundborg, G. Autologous tendons used as grafts for bridging peripheral nerve defects. J Hand Surg Br **24,** 284, 1999.
21. Bell, J., and Haycock, J.W. Next generation nerve guides—materials, fabrication, growth factors and cell delivery. Tissue Eng Part B Rev **8,** 116, 2012.
22. Ao, Q., Fung, C.K., Tsui, A.Y., Cai, S., Zuo, H.C., Chan, Y.S., and Shum, D.K. The regeneration of transected sciatic nerves of adult rats using chitosan nerve conduits seeded with bone marrow stromal cell-derived Schwann cells. Biomaterials **32,** 787, 2011.
23. Harvey, A.R., Chen, M., Plant, G.W., and Dyson, S.E. Regrowth of axons within Schwann cell-filled polycarbonate tubes implanted into the damaged optic tract and cerebral cortex of rats. Restor Neurol Neurosci **6,** 221, 1994.
24. Hsu, S.H., Su, C.H., and Chiu, I.M. A novel approach to align adult neural stem cells on micropatterned conduits for peripheral nerve regeneration: a feasibility study. Artif Organs **33,** 26, 2009.
25. Marchesi, C., Pluderi, M., Colleoni, F., Belicchi, M., Meregalli, M., Farini, A., Parolini, D., Draghi, L., Fruguglietti, M.E., Gavina, M., Porretti, L., Cattaneo, A., Battistelli, M., Prelle, A., Moggio, M., Borsa, S., Bello, L., Spagnoli, D., Gaini, S.M., Tanzi, M.C., Bresolin, N., Grimoldi, N., and Torrente, Y. Skin-derived stem cells transplanted into resorbable guides provide functional nerve regeneration after sciatic nerve resection. Glia **55,** 425, 2007.
26. Lundborg, G., Dahlin, L.B., Danielsen, N., Gelberman, R.H., Longo, F.M., Powell, H.C., and Varon, S. Nerve regeneration in silicone chambers: influence of gap length and of distal stump components. Exp Neurol **76,** 361, 1982.
27. Brown, R., Pedowitz, R., Rydevik, B., Woo, S., Hargens, A., Massie, J., Kwan, M., and Garfin, S.R. Effects of acute graded strain on efferent conduction properties in the rabbit tibial nerve. Clin Orthop Relat Res **296,** 288, 1993.
28. Kwan, M.K., Wall, E.J., Massie, J., and Garfin, S.R. Strain, stress and stretch of peripheral nerve. Rabbit experiments *in vitro* and *in vivo*. Acta Orthop Scand **63,** 267, 1992.
29. Rydevik, B.L., Kwan, M.K., Myers, R.R., Brown, R.A., Triggs, K.J., Woo, S.L., and Garfin, S.R. An *in vitro* mechanical and histological study of acute stretching on rabbit tibial nerve. J Orthop Res **8,** 694, 1990.
30. Phillips, J.B., Smit, X., De Zoysa, N., Afoke, A., and Brown, R.A. Peripheral nerves in the rat exhibit localized heterogeneity of tensile properties during limb movement. J Physiol **557,** 879, 2004.
31. Wright, T.W., Glowczewskie, F., Wheeler, D., Miller, G., and Cowin, D. Excursion and strain of the median nerve. J Bone Joint Surg Am **78,** 1897, 1996.
32. Wright, T.W., Glowczewskie, F., Jr., Cowin, D., and Wheeler, D.L. Ulnar nerve excursion and strain at the elbow and wrist associated with upper extremity motion. J Hand Surg Am **26,** 655, 2001.
33. Anava, S., Greenbaum, A., Ben Jacob, E., Hanein, Y., and Ayali, A. The regulative role of neurite mechanical tension in network development. Biophys J **96,** 1661, 2009.
34. Abe, I., Ochiai, N., Ichimura, H., Tsujino, A., Sun, J., and Hara, Y. Internodes can nearly double in length with gradual elongation of the adult rat sciatic nerve. J Orthop Res **22,** 571, 2004.
35. Bray, D. Axonal growth in response to experimentally applied mechanical tension. Dev Biol **102,** 379, 1984.
36. Bueno, F.R., and Shah, S.B. Implications of tensile loading for the tissue engineering of nerves. Tissue Eng Part B Rev **14,** 219, 2008.
37. Pfister, B.J., Iwata, A., Meaney, D.F., and Smith, D.H. Extreme stretch growth of integrated axons. J Neurosci **24,** 7978, 2004.
38. Topp, K.S., and Boyd, B.S. Structure and biomechanics of peripheral nerves: nerve responses to physical stresses and implications for physical therapist practice. Phys Ther **86,** 92, 2006.
39. Zheng, J., Lamoureux, P., Santiago, V., Dennerll, T., Buxbaum, R.E., and Heidemann, S.R. Tensile regulation of axonal elongation and initiation. J Neurosci **11,** 1117, 1991.
40. Rupp, A., Schmahl, W., Lederer, W., and Matiasek, K. Strain differences in the branching of the sciatic nerve in rats. Anat Histol Embryol **36,** 202, 2007.
41. Strasberg, J.E., Strasberg, S., Mackinnon, S.E., Watanabe, O., Hunter, D.A., and Tarasidis, G. Strain differences in

peripheral-nerve regeneration in rats. J Reconstr Microsurg **15,** 287, 1999.
42. Naples, G.G., Mortimer, J.T., Scheiner, A., and Sweeney, J.D. A spiral nerve cuff electrode for peripheral nerve stimulation. IEEE Trans Biomed Eng **35,** 905, 1988.
43. Oh, S.H., Kim, J.H., Song, K.S., Jeon, B.H., Yoon, J.H., Seo, T.B., Namgung, U., Lee, I.W., and Lee, J.H. Peripheral nerve regeneration within an asymmetrically porous PLGA/Pluronic F127 nerve guide conduit. Biomaterials **29,** 1601, 2008.
44. Nagata, Y., and Burger, M.M. Wheat germ agglutinin. Molecular characteristics and specificity for sugar binding. J Biol Chem **249,** 3116, 1974.
45. Oh, S.H., and Lee, J.H. Fabrication and characterization of hydrophilized porous PLGA nerve guide conduits by a modified immersion precipitation method. J Biomed Mater Res A **80,** 530, 2007.
46. McDonald, D.S., and Bell, M.S. Peripheral nerve gap repair facilitated by a dynamic tension device. Can J Plast Surg **18,** e17, 2010.
47. Rivlin, M., Sheikh, E., Isaac, R., and Beredjiklian, P.K. The role of nerve allografts and conduits for nerve injuries. Hand Clin **26,** 435, 2010.
48. Millesi, H. Reappraisal of nerve repair. Surg Clin North Am **61,** 321, 1981.
49. Millesi, H. The nerve gap. Theory and clinical practice. Hand Clin **2,** 651, 1986.
50. Flores, A.J., Lavernia, C.J., and Owens, P.W. Anatomy and physiology of peripheral nerve injury and repair. Am J Orthop (Belle Mead NJ) **29,** 167, 2000.
51. Lundborg, G. Intraneural microcirculation. Orthop Clin North Am **19,** 1, 1988.
52. Clark, W.L., Trumble, T.E., Swiontkowski, M.F., and Tencer, A.F. Nerve tension and blood flow in a rat model of immediate and delayed repairs. J Hand Surg Am **17,** 677, 1992.
53. Driscoll, P.J., Glasby, M.A., and Lawson, G.M. An *in vivo* study of peripheral nerves in continuity: biomechanical and physiological responses to elongation. J Orthop Res **20,** 370, 2002.
54. Sunderland, I.R., Brenner, M.J., Singham, J., Rickman, S.R., Hunter, D.A., and Mackinnon, S.E. Effect of tension on nerve regeneration in rat sciatic nerve transection model. Ann Plast Surg **53,** 382, 2004.
55. Smith, D.H., Wolf, J.A., and Meaney, D.F. A new strategy to produce sustained growth of central nervous system axons: continuous mechanical tension. Tissue Eng **7,** 131, 2001.
56. Abe, I., Tsujino, A., Hara, Y., Ichimura, H., and Ochiai, N. Paranodal demyelination by gradual nerve stretch can be repaired by elongation of internodes. Acta Neuropathol (Berl) **104,** 505, 2002.
57. Abe, I., Tsujino, A., Hara, Y., and Ochiai, N. Effect of the rate of prestretching a peripheral nerve on regeneration potential after transection and repair. J Orthop Sci **8,** 693, 2003.
58. Bora, F.W., Jr., Richardson, S., and Black, J. The biomechanical responses to tension in a peripheral nerve. J Hand Surg [Am] **5,** 21, 1980.
59. Ichimura, H., Shiga, T., Abe, I., Hara, Y., Terui, N., Tsujino, A., and Ochiai, N. Distribution of sodium channels during nerve elongation in rat peripheral nerve. J Orthop Sci **10,** 214, 2005.
60. Ikeda, K., Tomita, K., and Tanaka, S. Experimental study of peripheral nerve injury during gradual limb elongation. Hand Surg **5,** 41, 2000.
61. Yokota, A., Doi, M., Ohtsuka, H., and Abe, M. Nerve conduction and microanatomy in the rabbit sciatic nerve after gradual limb lengthening-distraction neurogenesis. J Orthop Res **21,** 36, 2003.
62. Li, J., and Shi, R. A device for the electrophysiological recording of peripheral nerves in response to stretch. J Neurosci Methods **154,** 102, 2006.
63. Jou, I.M., Lai, K.A., Shen, C.L., and Yamano, Y. Changes in conduction, blood flow, histology, and neurological status following acute nerve-stretch injury induced by femoral lengthening. J Orthop Res **18,** 149, 2000.
64. Lee, C., Ma, J., Deal, D.N., Smith, B.P., Koman, L.A., Smith, T.L., and Shilt, J.S. Neuromuscular recovery after distraction osteogenesis at different frequencies in a rabbit model. J Pediatr Orthop **26,** 628, 2006.
65. Spiegel, D.A., Seaber, A.V., Chen, L.E., and Urbaniak, J.R. Recovery following stretch injury to the sciatic nerve of the rat: an *in vivo* study. J Reconstr Microsurg **9,** 69, 1993.
66. Bruggeman, J.P., de Bruin, B.J., Bettinger, C.J., and Langer, R. Biodegradable poly(polyol sebacate) polymers. Biomaterials **29,** 4726, 2008.
67. Hwang, C.M., Khademhosseini, A., Park, Y., Sun, K., and Lee, S.H. Microfluidic chip-based fabrication of PLGA microfiber scaffolds for tissue engineering. Langmuir **24,** 6845, 2008.
68. Zhao, L., He, C., Gao, Y., Cen, L., Cui, L., and Cao, Y. Preparation and cytocompatibility of PLGA scaffolds with controllable fiber morphology and diameter using electrospinning method. J Biomed Mater Res B Appl Biomater **87,** 26, 2008.
69. Nishiura, Y., Hara, Y., Yoshii, Y., and Ochiai, N. Simultaneous gradual lengthening of both proximal and distal nerve stumps for repair of peripheral nerve defect in rats. Muscle Nerve **38,** 1474, 2008.
70. Sharula, Hara, Y., Nishiura, Y., Saijilafu, Kubota, S., and Ochiai, N. Repair of the sciatic nerve defect with a direct gradual lengthening of proximal and distal nerve stumps in rabbits. Plast Reconstr Surg **125,** 846, 2010.
71. Yamada, Y., Nishiura, Y., Saijilafu, Hara, Y., Ichimura, H., Yoshii, Y., and Ochiai, N. Repair of peripheral nerve defect by direct gradual lengthening of the distal nerve stump in rats: cellular reaction. Scand J Plast Reconstr Surg Hand Surg **43,** 297, 2009.

Address correspondence to:
Sameer B. Shah, PhD
Department of Orthopaedic Surgery and Bioengineering
University of California, San Diego
9500 Gilman Drive
Mail Code 0863
La Jolla, CA 92093

E-mail: sbshah@ucsd.edu

Received: January 16, 2012
Accepted: October 23, 2012
Online Publication Date: December 21, 2012